Rivista Italiana di Paleontologia e Stratigrafia
(*Research in Paleontology and Stratigraphy*)
vol. 132(2): 513-540. **July 2026**
DOI: https://doi.org/10.54103/2039-4942/30891

LOWER PLIOCENE FISH OTOLITHS FROM THE CABARRUYAN ISLAND, NORTHERN PHILIPPINES

DOMINIQUE P. MEDIODIA[1,2,3,4], LORRIE ANNE S. TORRALBA[5], JOHN PHILLIP R. BAGUIO[5], LEOPOLDO P. DE SILVA, JR.[5], ALLAN GIL S. FERNANDO[5] & CHIEN-HSIANG LIN[1,*]

[1]Biodiversity Research Center, Academia Sinica, Taipei 11529, Taiwan. E-mail: dpmediodia@up.edu.ph (DPM), chlin.otolith@gmail.com (C-HL)
[2]Biodiversity Program, Taiwan International Graduate Program, Academia Sinica and National Taiwan Normal University, Taipei 11529, Taiwan
[3]Department of Life Science, National Taiwan Normal University, Taipei 11677, Taiwan
[4]Institute of Marine Fisheries and Oceanology, College of Fisheries and Ocean Sciences, University of the Philippines Visayas, Philippines
[5]Nannoworks Laboratory, National Institute of Geological Sciences, College of Science, University of the Philippines Diliman, Quezon City, 1101, Philippines. E-mail: lstorralba@up.edu.ph (LAST), jrbaguio@up.edu.ph (JPB), lpdesilva@up.edu.ph (LPdS), asfernando@up.edu.ph (AGSF)
*Corresponding author.

Associate Editor: Giorgio Carnevale.

To cite this article: Mediodia D.P., Torralba L.A.S., Baguio J.P.R., De Silva L.P., Jr., Fernando A.G.S. & Lin C.-H. (2026) - Lower Pliocene fish otoliths from the Cabarruyan Island, Northern Philippines. *Rivista Italiana di Paleontologia e Stratigrafia*, vol. 132(2): 513-540.

Keywords: Fossil fishes; West Pacific; ichthyology; biodiversity.

Abstract: Fish otoliths are commonly found in the fossil record and are crucial for reconstructing past environments, especially in areas such as the Philippines, where well-preserved fish fossils are rare. This study analyzed fish otoliths from the Lower Pliocene clastic unit in Cabarruyan Island, northwestern Luzon Island, Philippines. The age of the sediments was constrained using calcareous nannofossil biostratigraphy, based on the last occurrence (LO) of *Reticulofenestra pseudoumbilicus* (Gartner, 1967) Gartner, 1969 and the first occurrence (FO) of *Pseudoemiliania lacunosa* Kamptner, 1963 ex Gartner, 1969. Bulk sediments were screen-washed, and individual otoliths were separated and identified. A total of 1,225 fish otoliths were analyzed, revealing 69 taxa in 28 families. We also report two new species: *Benthosema rarang* sp. nov. and *Myctophum luzonicum* sp. nov., as well as new fossil otolith records from the Philippines. The fish assemblage was dominated by the families Myctophidae, Sternoptychidae, Bregmacerotidae, Macrouridae, and Gobiidae, which agrees with findings from a previous study. The dominance of these families indicates an open marine environment and a tropical-to-subtropical climate during the Pliocene. The co-occurrence of deep- and shallow-water taxa in our study, together with other recorded fossils (e.g., fish vertebrae and scales, sea urchins, brachiopods, and other mollusks), suggests an outer-shelf-to-upper-slope paleoenvironment. This study not only provides an accurate age constraint for the marine sediments in Cabarruyan Island but also offers a significant opportunity to deepen our understanding of fish paleodiversity in the tropical West Pacific.

Received: February 16, 2026 accepted: June 12, 2026

Introduction

Cabarruyan Island (Anda, Pangasinan), located along the western margin of Lingayen Gulf in northwestern Luzon Island, northern Philippines, is geologically and paleontologically significant due to the presence of several fossiliferous sedimentary units that have yielded both marine and terrestrial vertebrate fossils (Beyer 1956 in de Ocampo 1983; von Koenigswald 1956 in de Ocampo 1983; Braches & Shutler 1984). Although the island's stratigraphy is still under revision, recent geological mapping and available micropaleontological age constraints suggest that a Pliocene clastic sedimentary unit and a Pliocene–Pleistocene limestone unit occur on the island and overlie older strata. Exposures of the clastic unit contain mollusks, elasmobranch teeth, and bony fish otoliths (Janssen 2007; Helwerda et al. 2014; van Hinsbergh & Helwerda 2019). Notably, the first record of fossil otoliths from the Philippines was from Cabarruyan Island and was attributed to the Santa Cruz Formation (van Hinsbergh & Helwerda 2019). However, the sampling design in that study was not described in detail to support quantitative comparisons of abundance, density, or diversity structure among samples.

Well-preserved, articulated fish skeletons are scarce in the Philippines (but see Přikryl et al. 2025), whereas isolated fish remains, such as teeth and otoliths, are comparatively abundant in marine sediments and can provide taxonomically informative records of fish assemblages (Mediodia et al. 2025). These offer a valuable opportunity to enhance our understanding of paleoichthyological diversity in the tropical West Pacific (Lin et al. 2021). In this study, we analyze an expanded otolith collection from the Lower Pliocene clastic unit of Cabarruyan Island. We revise, wherever necessary, the identifications reported by van Hinsbergh and Helwerda (2019) based on our expanded collection. Additionally, we refine age constraints using new calcareous nannofossil and planktonic foraminifera biostratigraphic analyses, thereby clarifying the age framework reported by van Hinsbergh and Helwerda (2019).

Geological setting

Cabarruyan Island (Anda, Pangasinan, northwestern Luzon Island) is situated within the Philippine Mobile Belt, a tectonically active area brought about by the collision of the Philippine Sea Plate, Eurasian Plate, and Indo-Australian Plate (Rangin 1991). The island is part of the Zambales Range Stratigraphic Group, which is mainly composed of ophiolitic and sedimentary formations of Mesozoic to Pleistocene age (Peña 2008; Mines & Geosciences Bureau [MGB] 2010). The island and the rest of western Pangasinan Province have been experiencing regional uplift since the Pliocene due to the subduction of the Scarborough Seamount Chain under the Manila Trench (Yang et al. 1996), reflected in the island's geology and stratigraphy (de Ocampo 1983).

De Ocampo (1983) describes a Pliocene clastic unit composed of interbedded marls, sandstones, siltstones, and claystones, mapped in mainland Pangasinan near Cabarruyan Island. The lowermost section consists of interbeds of sandstones and calcareous siltstones, while the middle section is composed of tuffaceous marls and claystones. In contrast, the uppermost section consists of interbedded calcareous sandstones and siltstones. The Bolinao Limestone, which consists of coralline limestones (de Ocampo 1983), conformably overlies the clastic unit. The contact is gradual, with interbeds of sandstones eventually transitioning into sandy limestone. De Ocampo (1983) provided no age data for the limestone but mapped most of the rocks on Cabarruyan Island as belonging to this formation. Overlying the Bolinao Limestone is the Zaragosa Mudstone, a highly fossiliferous Lower Pleistocene mudstone based on the gastropod assemblage (de Ocampo 1983). The youngest unit on the island is the "limestone conglomerate", which is a matrix-supported conglomerate composed of granule- to cobble-sized limestone and oyster shell clasts held together by a friable clay matrix. This unit was assigned a Middle Pleistocene age based on proboscidean fossils (Beyer 1956 in de Ocampo 1983; Von Koenigswald 1956 in de Ocampo 1983).

Geological mapping by the Bureau of Mines and Geosciences (BMG 1985) suggests that the island is underlain by the Upper Miocene Santa Cruz Formation, which consists of bedded to massive coralline limestones. Dimalanta et al. (2015) assigned an age of Late Miocene to Early Pliocene for the Santa Cruz Formation based on foraminiferal assemblages. In this study, the otolith-bearing horizons are from clastic sediments exposed on Cabar-

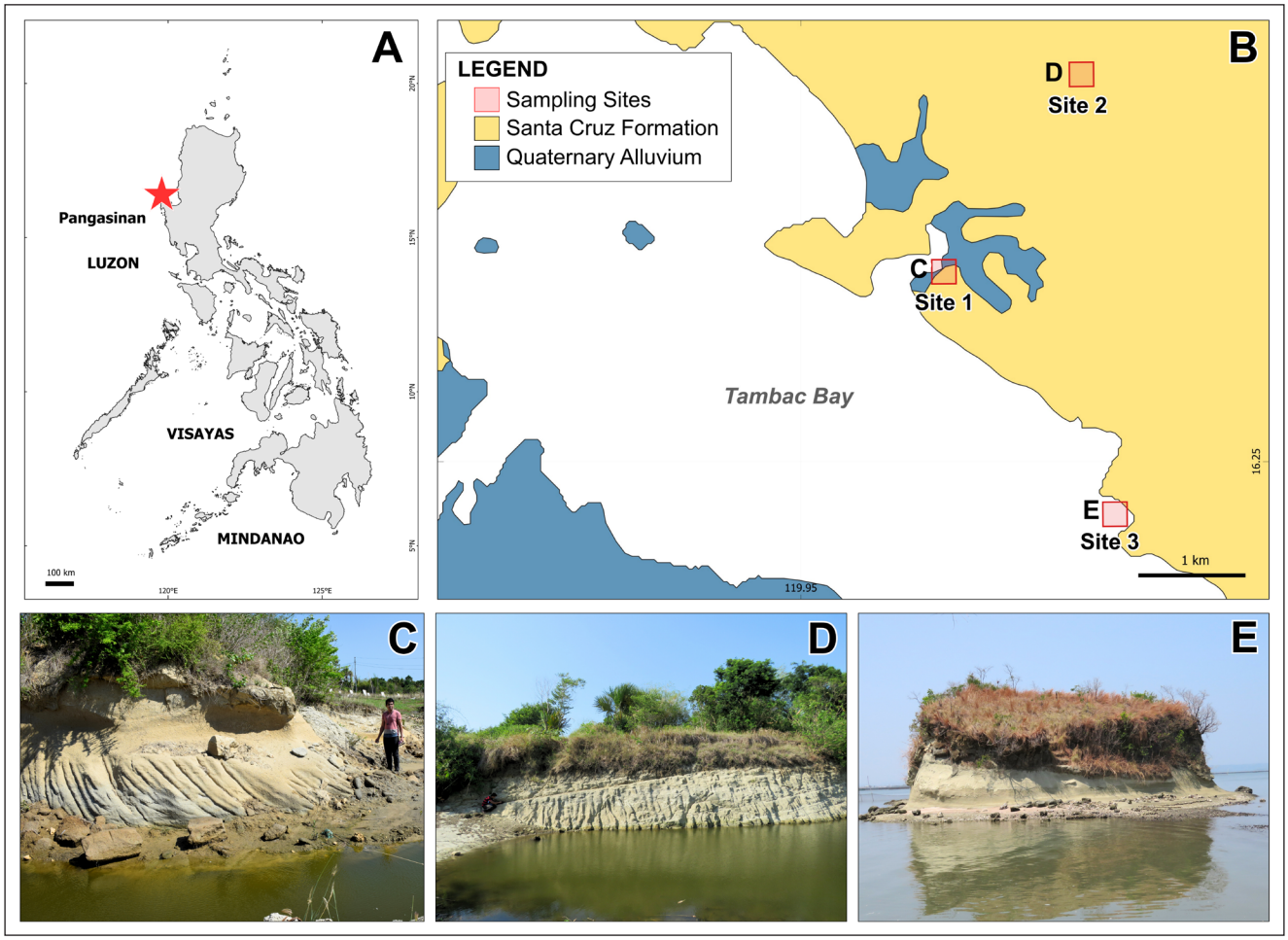

Fig. 1 - Map showing the sampling sites. A) geographic location of Pangasinan, northern Luzon. B) geologic map of Anda, Pangasinan, and surrounding areas adopted from the BMG Geological Survey Division (1985a, 1985b) (see "Sampling sites and micropaleontological biostratigraphy" section for discussion of geology and stratigraphy). C–E) actual photos of the Pliocene clastic unit exposures in Site 1 (Rarang Fishpond, Awile, Cabarruyan Island, Anda) (C), Site 2 (Namagbagan Dam, Cabarruyan Island, Anda) (D), and Site 3 (Pusong Island, Macandocandong, Cabarruyan Island, Anda) (E).

ruyan Island. Although van Hinsbergh and Helwerda (2019) referred their otoliths to clastic sediments of the Santa Cruz Formation, more recent geological mapping and micropaleontological constraints indicate that the material was more likely derived from the Pliocene clastic unit, which is also widely exposed in western Pangasinan (A. G. S. Fernando, pers. comm. 2025). We therefore use "Pliocene clastic unit" here as a working term for the otolith-bearing strata (see below, under site description).

Material and methods

Sampling sites and micropaleontological biostratigraphy

Bulk sediment samples were collected from three sites on Cabarruyan Island, northwestern Luzon Island, Philippines (Fig. 1) in March 2023 (77.83 kg), and from Site 1 in October 2025 (8.69 kg). Actual sediment weights per sample are provided in Tab. S1. Calcareous nannofossils in the sampled sediments are moderately to well-preserved, enabling detailed biostratigraphic analysis.

The sediment ages for the three sites were constrained using calcareous nannofossil datums, specifically the last occurrence (LO) of *Reticulofenestra pseudoumbilicus* and the first occurrence (FO) of *Pseudoemiliania lacunosa*, both key biostratigraphic markers of the Early Pliocene interval. Planktonic foraminifera were analyzed from the Namagbagan Dam sample only (Site 2). The sample contains *Globorotalia margaritae*, an index species with a relatively short stratigraphic range in tropical-to-temperate seas (Bolli 1970; Srinivasan et al. 1981). The LO of *G. margaritae* occurs at the top of Zone PL2 (3.85

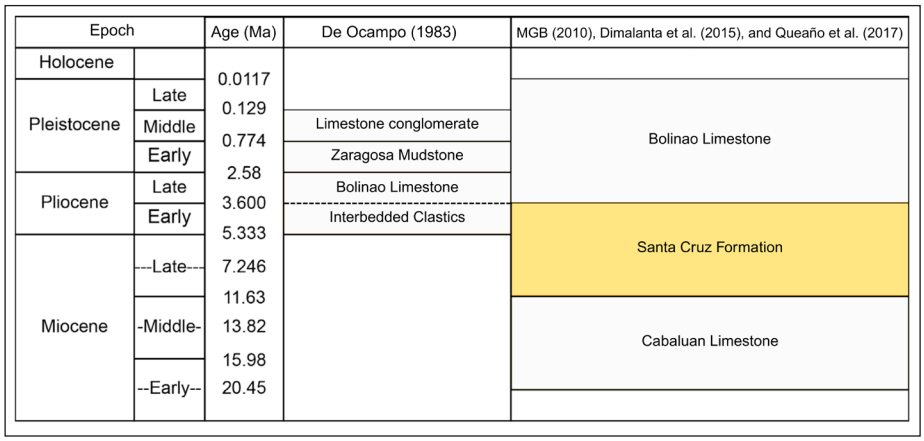

Fig. 2 - Comparative stratigraphic columns of Cabarruyan Island and western Pangasinan. Left: De Ocampo (1983). Right: MGB (2010), Dimalanta et al. (2015) & Queaño et al. (2017). The studied formation (Santa Cruz Formation) is indicated in yellow.

Ma), consistent with a late Early Pliocene age assignment and concordant with the calcareous nannofossil constraints.

Based on these nannofossil and planktonic foraminifera data, the fossiliferous fine-grained clastic strata (siltstone/mudstone) on the island are assigned to late Early Pliocene age. This correlates with the Pliocene unit identified by de Ocampo (1983) in mainland Pangasinan. No detailed micropaleontological analysis has been done for the fine-grained clastic unit on the island. MGB (1985) mapped the island as underlain by the Upper Miocene Santa Cruz Formation, whose age was extended by Dimalanta et al. (2015) to the Early Pliocene (Fig. 2). Whether the otolith-bearing clastic unit should be assigned to the Santa Cruz Formation or treated as a separate, unnamed Pliocene unit remains unresolved. Ongoing stratigraphic revisions are expected to refine this framework (Baguio et al. 2025).

- **Site 1** (Rarang Fishpond, Brgy. Awile, Cabarruyan Island, Anda, Pangasinan; Fig. 1C).

Location (GPS coordinates): 16°15'58"N, 119°57'40"E.
Stratigraphy: Unnamed Pliocene clastic unit in Cabarruyan Island.
Lithology: Medium-grained sandstone.
Calcareous nannofossil zone: NN15 (Lower Pliocene) based on the presence of *Discoaster pentaradiatus*, *Pseudoemiliania lacunosa*, and *Reticulofenestra haqii*
Available material: Sixteen bulk samples (~3 kg each), weighing 48.85 kg.

- **Site 2** (Namagbagan Dam, Cabarruyan Island, Anda, Pangasinan; Fig. 1D).

Location (GPS coordinates): 16°17'02"N, 119°58'29"E.
Stratigraphy: Unnamed Pliocene clastic unit in Cabarruyan Island.
Lithology: Siltstone.
Calcareous nannofossil zone: NN15 (Lower Pliocene) based on the presence of *D. pentaradiatus*, *P. lacunosa*, *R. haqii*, *Reticulofenestra pseudoumbilicus*, and *Sphenolithus abies*.
Available material: Nine bulk samples (~3 kg each), weighing 27.37 kg.

- **Site 3** (Pusong Island, Brgy. Macandocandong, Cabarruyan Island, Anda, Pangasinan; Fig. 1E).

Location (GPS coordinates): 16°14'43"N, 119°58'41"E.
Stratigraphy: Unnamed Pliocene clastic unit in Cabarruyan Island.
Lithology: Siltstone.
Calcareous nannofossil zone: NN15 (Lower Pliocene) based on the presence of *D. pentaradiatus*, *P. lacunosa*, *R. haqii*, *R. pseudoumbilicus*, and *S. abies*.
Available material: Five bulk samples (~3 kg each), weighing 14.57 kg.

Otolith processing, identification, and diversity analyses

All sediment samples were first immersed in water and wet-sieved using a 500-µm mesh. The retained residues were oven-dried overnight at 40 °C, and otoliths larger than 500-µm were hand-picked under a stereomicroscope. Representative otoliths were imaged with a digital camera mounted on a stereomicroscope. Stacked images were processed using Helicon Focus software, and the figures were prepared and enhanced in Adobe Photoshop.

For otolith identification, we consulted Smale et al. (1995), Rivaton and Bourret (1999), Schwarzhans (1999, 2013), Aguilera and de Aguilera (2001), Schwarzhans and Aguilera (2013), Lin and Chang (2012), Nolf (2013), van Hinsbergh and Helwerda (2019), Mitsui et al. (2021, 2023), Lin et al. (2023), and Chew et al. (2025). In addition, specimens were directly compared with an in-house reference collection of extant otoliths housed at the Biodiversity Research Museum, Academia Sinica, Taiwan (BRCAS) under catalogue code CHLOL.

All collected materials are stored at the Nannoworks Laboratory, National Institute of Geological Sciences, University of the Philippines Diliman, Philippines (NIGS). Holotypes are deposited at the National Museum of the Philippines – Museum of Natural History under the registration numbers NMP-2523 and NMP-2524. The paratypes are deposited in NIGS under NIGSPAL-FISH-013–15, and at the Biodiversity Research Museum, Academia Sinica under ASIZF0101147–49.

We quantified otolith abundance in the sediments by calculating otolith density, defined as the number of otoliths per kilogram of dry sediment for each sample, following Lin et al. (2023). Results were visualized using *ggplot2* package, and differences among samples were evaluated using the Kruskal–Wallis test followed by Dunn's post hoc test with Holm adjustment in R. Otolith diversity was assessed using Hill numbers (Hill 1973), calculated for three orders: q = 0 (${}^0D$, species richness), q = 1 (${}^1D$, Shannon diversity, reflecting abundant species), and q = 2 (${}^2D$, Simpson diversity, reflecting dominant species) (Chao et al. 2014). Because Hill numbers depend on sample coverage, we estimated diversity using specimen-based rarefaction, which provides coverage-standardized diversity estimates (Chao & Jost 2012; see also Lin et al. 2023). Confidence intervals (95%) were derived from 300 bootstrap replicates (Hsieh et al. 2016), and rarefaction curves were generated using the *iNEXT* package in R (Chao et al. 2014; Hsieh et al. 2016). Rank-abundance plots (log-transformed) were used to summarize taxonomic composition and relative abundance (Lin et al. 2023; Lin & O'Dea 2025). Diversity indices in this study were not compared with those of van Hinsbergh and Helwerda (2019) because the sampling approach and processing protocols in that study were not documented, making any quantitative comparison potentially misleading.

Results

Systematic paleontology

A list of identified taxa and their abundance is presented in Tab. 1. We adhere to the classification scheme of Nelson et al. (2016). For Acropomatiformes, we follow Davis et al. (2016). Authorship follows van der Laan et al. (2014) and Fricke et al. (2025). We use the term "otolith" to refer to the saccular otolith (sagitta) unless stated otherwise. General otolith terminology follows Lin and Chang (2012), Nolf (2013), and Schwarzhans (2013). Given that many otolith-based taxa from neighboring regions have been described in detail in recent works (Schwarzhans & Ohe 2019; van Hinsbergh & Helwerda 2019; Schwarzhans et al. 2022; Lin et al. 2023), we provide brief remarks for common taxa, focusing on diagnostic features and any deviations from published material. Full descriptions are provided for the new species reported in this study.

Morphometric and measurement data include otolith length (OL), otolith height (OH), ostium length (OsL), and cauda length (CaL), measured using ImageJ. Synonymy lists are limited only to nominal species and relevant records from the Philippines.

Order **Anguilliformes** Regan, 1909
Family Congridae Kaup, 1856
Genus *Ariosoma* Swainson, 1838

***Ariosoma* sp.**
Fig. 3A

Remarks. A single otolith attributable to *Ariosoma* was recovered. It is circular to broadly oval in outline, thick, and compact, with a low central swelling on the dorsal field (OL = 2.32 mm; OH = 2.06 mm; OL/OH = 1.13). The sulcus is short, shallow, and undivided, positioned near the center. The S-shaped sulcus with short, dorsally oriented ostial channel is a key diagnostic feature for *Ariosoma* (Schwarzhans 2019; Lin et al. 2021: figs. 4a–f; Lin et al. 2024: fig. 4A; Ng et al. 2024: figs. 12G, I). Our specimen resembles otoliths of the extant *Ariosoma indicum* Kodeeswaran et al. 2022 (see Fig. S1A). However, we have only one slightly eroded specimen, which limits our description. Thus, we leave it as *Ariosoma* sp. Although van Hinsbergh and Helwerda (2019: pl. 1, fig. 1; OL/OH = 1.06 mm) also reported *Ariosoma* sp., the figured specimen differs in overall outline from ours, suggesting the presence of at least two morphotypes within the assemblage.

Order **Siluriformes** Cuvier, 1817
Family Plotosidae Bleeker, 1858
Genus *Plotosus* Lacepède, 1803

Plotosus lineatus (Thunberg, 1787)
Fig. 3B

Remarks. A single otolith (lapillus) of *Plotosus lineatus* was recovered. It is thick and nearly circular, with rounded, weakly crenulate margins. The inner face is gently convex with a low central umbo, whereas the outer face is flat to slightly concave. It shows a posteriorly opening groove consistent with plotosid morphology (Rivaton & Bourret 1999: pl.

Tab. 1 - List of otolith-based fish taxa from Early Pliocene Cabarruyan Island, Pangasinan, northern Luzon, Philippines.

Family/Order	Taxa	No. of otoliths in this study	Figure	van Hinsbergh & Helwerda 2019 (revised count, original attribution)
Congridae	*Ariosoma* sp.	1	Fig. 3A	1
	Bathycongrus sp.			3
	Congridae indet.	4		
Gonorynchidae	*Gonorynchus abbreviatus*			1
Plotosidae	*Plotosus lineatus*	1	Fig. 3B	
Argentinidae	*Glossanodon semifasciatus*	1	Fig. 3C	
	Argentina sp.			1
Opisthoproctidae	*Monacoa grimaldii*			1, *Opisthoproctus grimaldii*
Gonostomatidae	Gonostomatidae indet.	1	Fig. 3D	
Sternoptychidae	*Maurolicus* cf. *muelleri*	6	Fig. 3E	24
	Maurolicus sp.	8		7
	Polyipnus aquavitus			9
	Polyipnus aff. *indicus*			2
	Polyipnus sp.	262	Fig. 3F–G	
	Valenciennellus tripunctulatus	15	Fig. 3H	1
Paraulopidae	*Paraulopus* cf. *brevirostris*			1
	Paraulopus sp.			5
Scopelarchidae	*Scopelarchus* sp.	3	Fig. 3I	
Myctophidae	*Benthosema fibulatum*			30
	Benthosema aff. *fibulatum*			55
	Benthosema parafibulatum	14	Fig. 4A–B	
	Benthosema rarang sp. nov.	34	Fig. 4C–G	
	Benthosema suborbitale	9	Fig. 4H	
	Benthosema sp.	1		
	Ceratoscopelus sp.	15	Fig. 5A	8
	Centrobranchus sp.	1	Fig. 5B	
	Dasyscopelus obtusirostris	7	Fig. 5C	
	Dasyscopelus selenops			1, *Myctophum spinosum*
	Dasyscopelus spinosus			1, *Myctophum spinosus*
	Diaphus adenomus	1	Fig. 6A	
	Diaphus aequalis			2
	Diaphus mollis	1	Fig. 6B	1
	Diaphus diademophilus	3	Fig. 6C	
	Diaphus aff. *garmani*			9
	Diaphus regani	42	Fig. 6D	3
	Diaphus splendidus	2	Fig. 6E	
	Diaphus sp. 1			1
	Diaphus sp. 2			1
	Diaphus sp.	29		19
	Diogenichthys atlanticus	2	Fig. 7A	
	Hygophum sp.	1	Fig. 7B	
	Dasyscopelus aff. *jacksoni*			1, *Lampadena* aff. *jacksoni*
	Lampadena dea	6	Fig. 7C	
	Lampadena sp.	3		
	Lampanyctus alatus	1	Fig. 7D	4
	Lampanyctus nobilis	1	Fig. 7E	1, *Lampanyctus alatus*
	Lampanyctus tenuiformis			2, *Lampanyctus alatus*
	Lobianchia dofleini	8	Fig. 8A	
	Lobianchia gemellarii			5
	Myctophum luzonicum sp. nov.	6	Fig. 8B–D	
	Myctophum sp.	5		3
	Taaningichthys sp.	2	Fig. 8E	
	Myctophidae indet.	333		229
Macrouridae	*Coelorinchus* cf. *australis*			10
	Coelorinchus sp.	2	Fig. 9A	
	Hymenocephalus aeger			7
	Hymenocephalus cf. *iwamotoi*	4	Fig. 9B	
	Hymenocephalus torvus	24	Fig. 9C	

7, figs. 3–4; Lin & Chang 2012: pl. 6, fig. 74; Nolf 2013: pl. 36).

Order **Argentiniformes** Johnson & Patterson, 1996

Family Argentinidae Bonaparte, 1846

Genus *Glossanodon* Guichenot, 1867

Glossanodon semifasciatus (Kishinouye, 1904)

Fig. 3C

Remarks. One elliptical-shaped otolith with a crenate dorsal margin and a smooth ventral margin was identified as *Glossanodon semifasciatus* (OL = 4.64, OH = 3.34, OL/OH = 1.38). The ventral rim is convex and angled towards the postero-dorsal region. The anterior region is nearly straight and smooth. Sulcus is median and horizontally oriented. The cauda is deep and elongated, but the ostium is damaged in our specimen. The ostial colliculum is deep, and the caudal colliculum is shallow. Crista superior is ridge-

Tab. 1 - List of otolith-based fish taxa from Early Pliocene Cabarruyan Island, Pangasinan, northern Luzon, Philippines.

Family/Order	Taxa	No. of otoliths in this study	Figure	van Hinsbergh & Helwerda 2019 (revised count, original attribution)
Macrouridae	*Hymenocephalus* sp.	21		
	Hymenogadus gracilis	14	Fig. 9D	
	Nezumia sp.	3	Fig. 9E	
	Ventrifossa sp.	1	Fig. 9F	
Bregmacerotidae	*Bregmaceros japonicus*	29	Fig. 10A	
	Bregmaceros cf. *mcclellandi*			16
	Bregmaceros nectabanus	52	Fig. 10B	
	Bregmaceros sp.	28		
Holocentridae	*Myripristis* sp.	1	Fig. 10C	
Diretmidae	*Diretmus argenteus*	1	Fig. 10D	
Carapidae	*Onuxodon* sp.	1	Fig. 10E	
	Carapidae indet.	1	Fig. 10F	2
Ophidiidae	*Neobythites* sp.	3	Fig. 10G	1
Bythitidae	*Saccogaster* sp.			3
	Bythitidae indet.	1	Fig. 10H	
Apogonidae	*Apogon* sp.			22
	Xeniamia atrithorax			2, Apogonidae indeterminate
	Apogonidae indet.	36	Fig. 11A–B	
Gobiidae	*Gobiopterus* sp.	6	Fig. 11C–D	1, Gobiidae indeterminate
	Priolepis sp.	1	Fig. 11E	5
	Suruga fundicola	3	Fig. 11F	38
	Gobiidae indet.	3	Fig. 11G	
Atherinidae	*Atherinomorus lacunosus*	1	Fig. 12A	
Belonidae	Belonidae indet.	1	Fig. 12B	
Carangidae	*Decapterus* sp.	1	Fig. 12C	
	Carangidae indet.			1
Gempylidae	*Diplospinus multistriatus*			1
	Gempylidae sp. 1			2, Gempilidae
	Gempylidae indet.	2	Fig. 12D	
Trichiuridae	*Trichiurus* sp.	1	Fig. 12E	
Champsodontidae	*Champsodon* sp.	2	Fig. 12F	1
Hemerocoetidae	*Pteropsaron* sp.			6
Bembropidae	*Bembrops* sp.			1, Brembropidae
Malakichthyidae	*Malakichthys* sp.			1, Sparidae indeterminate
Synagropidae	*Parascombrops schwarzhansi*	8	Fig. 13A	19
	Parascombrops aff. *serratospinosus*			2
	Parascombrops sp.	3	Fig. 13B	
Bathyclupeidae	*Bathyclupea* sp.			2
Serranidae	Serranidae indet.			6
	Eupercaria indet. 1			1
	Eupercaria indet. 2			1
Leiognathidae	*Equulites* sp.	1	Fig. 13C	
Cepolidae	*Owstonia nigromarginata*			6, *Owstonia nigromarginatus*
	Owstonia sp.			2
	Cepolidae indet.	2	Fig. 13D	
Triglidae	*Satyrichthys* sp.	2	Fig. 13E	
Scorpaeniformes	Scorpaeniformes indet.	3	Fig. 13F	
Acanthuridae	Acanthuridae indet.	2	Fig. 13G	
Sparidae	Sparidae indet.			2
Caproidae	*Antigonia capros*			2
	Utricular otoliths	5		2
	Indeterminate	127		
		1225		597

like and crista inferior is well-developed (Smale et al. 1995: pl. 9, fig. E; Lin & Chang 2012: pl. 7, 75; Mitsui et al. 2021: fig. 4O). The overall morphology of *G. semifasciatus* is similar to *Argentina kagoshimae* (Jordan & Snyder, 1902), but *A. kagoshimae* has a lower OL/RL ratio (2.4–2.7) than *G. semifasciatus* (3.1–3.4; Ohe et al. 1985). Unfortunately, the anterior region of our specimen is damaged, which limits our description of rostrum length. However, the fossil otolith closely resembles the extant otoliths of *G. semifasciatus* in our comparative collection than *A. kagoshimae*, particularly in the structure of the dorso-posterior rim and the curved ventral rim (vs. the flatter ventral rim in *A. kagoshimae*; see Figs. S1B–C). Accordingly, we assign the specimen as *G. semifasciatus*.

Order **Stomiiformes** Regan, 1909
Family Gonostomatidae Cocco, 1838
Gonostomatidae indet.

Fig. 3D

Remarks. A single gonostomatid otolith with a subcircular to broadly oval shape, a narrow sulcus, and poorly developed crista is typical of gonostomatid otoliths. The overall discoid form and the semi-rounded posterior rim resemble those of the extant gonostomatid *Sigmops elongatus* (Günther, 1878), as figured in Ng et al. (2024; fig. 16B). However, our specimen has a broken anterior rim, which obscures key features required for a reliable genus-level diagnosis.

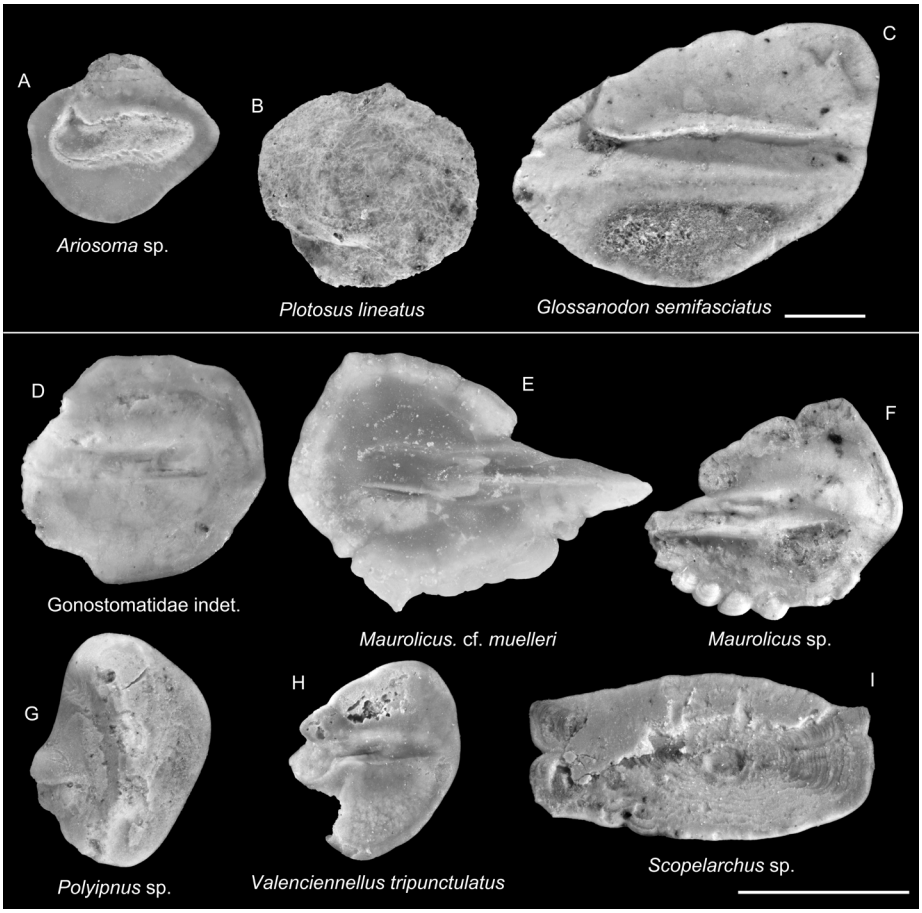

Fig. 3 - Otoliths from Early Pliocene marine sediments in Cabarruyan Island, northwestern Luzon Island, Philippines. Scale bars = 1 mm. Images are inner views unless otherwise indicated. A) *Ariosoma* sp., NIGSPAL-FISH-016. B) *Plotosus lineatus* (Thunberg, 1787), NIGSPAL-FISH-018, C) *Glossanodon semifasciatus* (Kishinouye, 1904), NIGSPAL-FISH-019, D) Gonostomatidae indet., NIGSPAL-FISH-020, E) *Maurolicus* cf. *muelleri*, NIGSPAL-FISH-021, F) *Maurolicus* sp., NIGSPAL-FISH-022, G) *Polyipnus* sp., NIGSPAL-FISH-023, H) *Valenciennellus tripunctulatus* (Esmark, 1871), NIGSPAL-FISH-024, I) *Scopelarchus* sp., NIGSPAL-FISH-025.

Family Sternoptychidae Duméril, 1805
Genus *Maurolicus* Cocco, 1838

Maurolicus **cf. *muelleri*** (Gmelin, 1789)

Fig. 3E

2019 *Maurolicus* cf. *muelleri*—van Hinsbergh & Helwerda, pl.1, figs. 9–13.

Remarks. Six small, thin otoliths with a teardrop outline were recovered. The inner faces are partially eroded, but the preserved sulcus is moderately long and narrow, with a widened ostium that grades into a straight and deep cauda. These combined features resemble *Maurolicus muelleri* (Gmelin, 1789) (Rivaton & Bourret 1999: pl. 93, figs. 13–16; Lin & Chang 2012: pl. 7, 75). However, because the anterior region of most of the specimens is not preserved, we retain the identification of van Hinsbergh and Helwerda (2019) as *Maurolicus* cf. *muelleri*.

Maurolicus **sp.**

Fig. 3F

Remarks. Eight specimens in our collection are assigned to the genus *Maurolicus*, based on overall otolith morphology (see remarks under *Maurolicus* cf. *muelleri*); however, these otoliths have a less sharply developed rostrum, and because most of the posterior region is damaged, we conservatively identify them as *Maurolicus* sp.

Genus *Polyipnus* Günther, 1887

Polyipnus **sp.**

Fig. 3G

?2019 *P. aquavitus* —van Hinsbergh & Helwerda, figs. 18–19.
?2019 *P.* aff. *indicus*—van Hinsbergh & Helwerda, fig. 20.

Remarks. A total of 262 otoliths attributable to *Polyipnus* were recovered. They exhibit an ear-like shape with a thick, smooth posterior margin and a horizontal cauda, consistent with *Polyipnus* otoliths (Lin et al. 2017: figs. C2, C4, D–E; Lin et al. 2023: figs. 4f–g). Some otoliths resemble those specimens in van Hinsbergh and Helwerda (2019: figs. 18–20; identified as *P. aquavitus* Baird, 1971 and fig. 20 as *P.* aff. *indicus*). However, due to the absence of diagnostic features at the species level and limited comparative material, we refrain from a more precise

taxonomic assignment and identify the material as *Polyipnus* sp. We further proposed reassignment of *P. aquavitus* (figs. 18–19) and *P.* aff. *indicus* (fig. 20) of van Hinsbergh & Helwerda (2019) to *Polyipnus* sp.

Genus *Valenciennellus* Jordan & Evermann, 1896

Valenciennellus tripunctulatus (Esmark, 1871)
Fig. 3H

2019 *Valenciennellus tripunctulatus*—van Hinsbergh & Helwerda, pl. 2, fig. 21.

Remarks. Fifteen oval-shaped otoliths with narrow and straight sulcus, flared ostium, and elongated cauda that constricts near the caudal rim resemble *Valenciennellus tripunctulatus* (Rivaton & Bourret 1999: pl. 97, figs. 12–19; Lin et al. 2017: figs. 4M–N; Mitsui et al. 2021: fig. 5A). Although all specimens are partially damaged, key diagnostic features remain visible and allow identification.

Order **Aulopiformes** Rosen, 1973
Family Scopelarchidae Alcock, 1896
Genus *Scopelarchus* Alcock, 1896

***Scopelarchus* sp.**
Fig. 3I

Remarks. Three otoliths were assigned to the genus *Scopelarchus* based on their moderately thin, rectangular outline, straight anterior rim, and curved posterior rim. They closely resemble *Scopelarchus analis* (Brauer, 1902) as illustrated in Smale et al. (1995: pl. 14, fig. F1) and Lin et al. (2017: fig. 4L). However, because the inner faces of all specimens are eroded, we retain the identification at the genus level pending additional material with intact inner-face features.

Order **Myctophiformes** Regan, 1911
Family Myctophidae Gill, 1893
Genus *Benthosema* Goode & Bean, 1896

Benthosema parafibulatum Lin, 2023
Figs. 4A–B

2019 *Benthosema* aff. *fibulatum*—van Hinsbergh & Helwerda, pl. 3, figs. 28–29, 31; non pl. 3, figs. 30, 32–35.
2023 *Benthosema parafibulatum*—Lin et al., figs. 6a–g.

Remarks. *Benthosema* otoliths are distinguished from other myctophid genera by 1–3 ventral denticles, a longer, more robust antirostrum, and a relatively longer ostium (Schwarzhans 2019; Schwarzhans & Ohe 2019; Lin et al. 2023). Nine oval otoliths with two prominent ventral denticles were identified as *Benthosema parafibulatum* (Lin et al. 2023: figs. 6a–g). These additional specimens support reassignments of van Hinsbergh & Helwerda's materials from *B.* aff. *fibulatum* to *B. parafibulatum* (see Lin et al. 2023 for full description).

***Benthosema rarang* sp. nov.** Mediodia & Lin
Figs. 4C–G

2019 *Benthosema* aff. *fibulatum*—van Hinsbergh & Helwerda, pl. 3, figs. 32, 34; non pl. 3, figs. 28–31, 33, 35.

Holotype: NMP-2523 Left sagitta (Fig. 4C), from Cabarruyan Island, Pangasinan, northwestern Luzon Island, Philippines
Paratypes: Four specimens: Two specimens NIGSPAL-FISH-013 and NIGSPAL-FISH-014 (Figs. 4D–E), two specimens ASIZF0101147–48 (Figs. 4F–G).
Etymology: The species name refers to Rarang Fishpond, Brgy. Awile, Pangasinan, the type locality where the specimens were collected.
Diagnosis: OL/OH = 1.17–1.22, OL/OT = 3.84–4.41. Dorsal rim flat and angled towards the posterior rim. Rostrum and antirostrum short and blunt with a shallow excisura.

Description. The otolith is discoid and moderately thick (1.61–1.85 mm length). The inner face is slightly concave and smooth. Dorsal rim angular with a distinctly flattened mid-dorsal section. Ventral rim convex with low, subdued crenulations rather than discrete ventral denticles. The posterior rim is curved and slightly blunt in the middle portion. The sulcus is straight, median-oriented, and slightly deep. Ostium is broad and flared. Cauda is slightly narrower than the ostium, tubular, and terminates before the posterior rim. It has a weak collum. The ostial colliculum is low and smooth, and the cauda colliculum is restricted to the central part of the cauda. The crista superior is well-developed, and the crista inferior is ridge-like and prominently located in the cauda. The rostrum is blunt and protruding. Antirostrum is blunt and short, creating a shallow excisura. A shallow dorsal depression is present.

Remarks. Otoliths of the new species are more compact (OL/OH = 1.17–1.22) than the otoliths of *B. parafibulatum* (OL/OH = 1.27). It further differs from *B. parafibulatum* in having a more angled anterodorsal rim. The flattened dorsal rim is a unique feature of *B. rarang* sp. nov. as compared to the

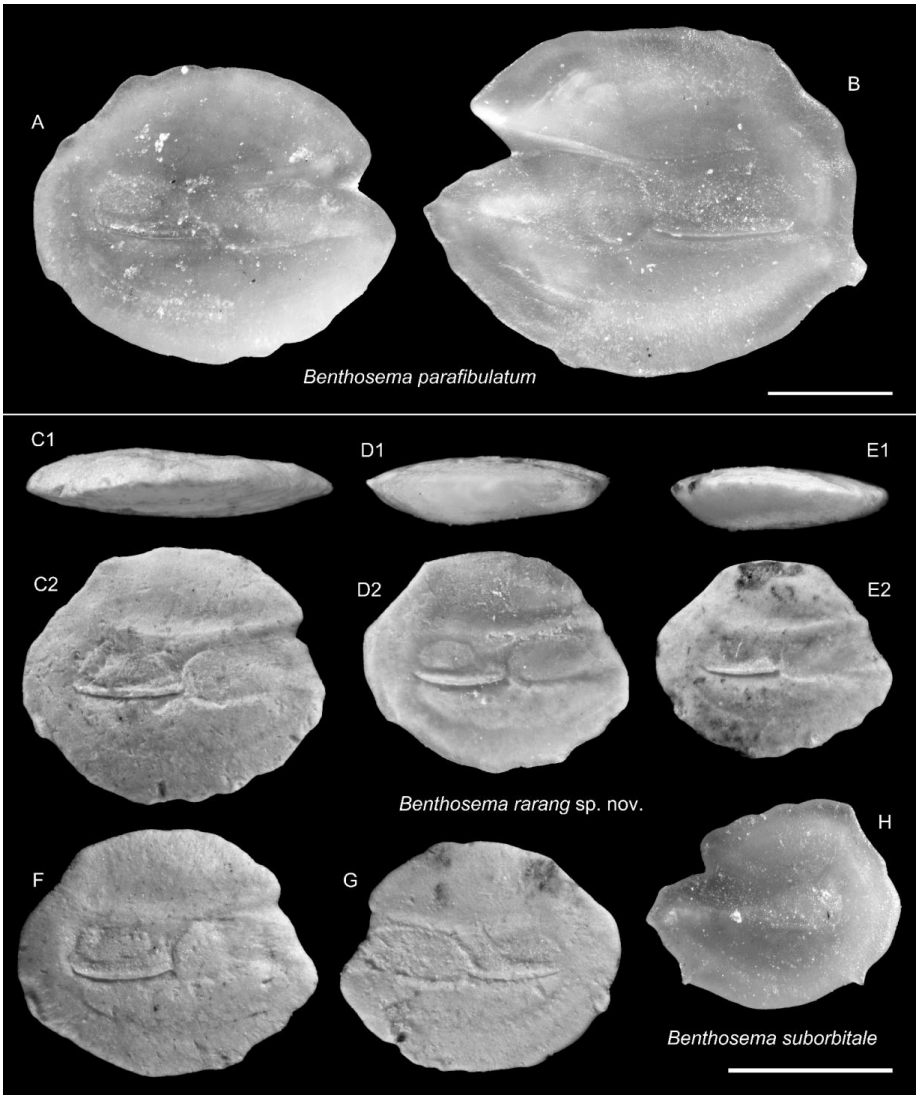

Fig. 4 - Otoliths from Early Pliocene marine sediments in Cabarruyan Island, northwestern Luzon Island, Philippines. Scale bars = 1 mm. Images are inner views unless otherwise indicated. A–B) *Benthosema parafibulatum* Lin, 2023, NIGSPAL-FISH-026, C–G) *Benthosema rarang* sp. nov., C – holotype, NMP-2523, D–G – paratypes, D–E) NIGSPAL-FISH-0213–14, D–G) ASIZF0101147–48, H) *Benthosema suborbitale* (Gilbert, 1913), NIGSPAL-FISH-028. 1, ventral view; 2, inner view.

crenulated with irregular denticles in species such as *B. parafibulatum* (Figs. 4A–B) and *B. suborbitale* (Fig. 4H). The *B. suborbitale* otoliths in our collection have a higher, more highly angled posterodorsal rim than those of the new species. We propose that the two otoliths identified as *B.* aff. *fibulatum* by van Hinsbergh & Helwerda (2019: pl. 3, figs. 31–32) also refer to *B. rarang* sp. nov. based on their closely matching overall morphology. There are 29 non-type specimens in the collection (NIGSPAL-FISH-027)

Occurrence: Currently known only from Cabarruyan Island, Pangasinan, northwestern Luzon Island, Philippines.

Benthosema suborbitale (Gilbert, 1913)

Fig. 4H

2023 *Benthosema suborbitale*—Lin et al., figs. 8a–b.

Remarks. Nine specimens in our collection were identified as *Benthosema suborbitale* (Gilbert, 1913) based on the depression on the posterodorsal rim and two prominent ventral rim denticle separated by a smooth gap (Schwarzhans 2019, fig. 49-4; Smale et al. 1995, pl. 16, fig. H; Mitsui et al. 2021, fig. 5B; Lin et al., figs. 8a–b.).

Genus *Ceratoscopelus* Günther, 1864

Ceratoscopelus sp.

Fig. 5A

Remarks. Fifteen otoliths resemble *Ceratoscopelus warmingii* based on their sesame-like otoliths, straight sulcus, and relatively protruding rostrum (van Hinsbergh & Helwerda 2019, pl. 4, figs. 39–40; Mitsui et al. 2021: fig. 5D, 2023: fig. 5a; Lin et al. 2023, figs. 8d–e). Our specimen also resembles the otoliths of *Ceratoscopelus townsendi* (Eigenmann & Eigenmann, 1889) (see Schwarzhans & Ohe 2019 for a full description). However, our specimens are all juveniles, so we conservatively identify our speci-

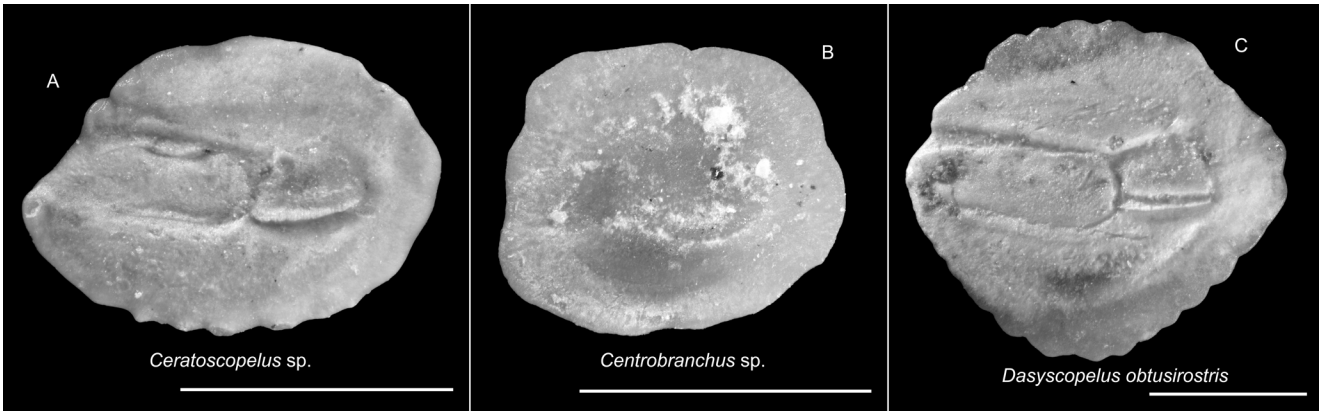

Fig. 5 - Otoliths from Early Pliocene marine sediments in Cabarruyan Island, northwestern Luzon Island, Philippines. Scale bars = 1 mm. Images are inner views unless otherwise indicated. A) *Ceratoscopelus* sp., NIGSPAL-FISH-030, B) *Centrobranchus* sp., NIGSPAL-FISH-031, C) *Dasyscopelus obtusirostris* (Tåning, 1928), NIGSPAL-FISH-032.

mens as *Ceratoscopelus* sp. until additional adult specimens are available.

Genus *Centrobranchus* Fowler, 1904

***Centrobranchus* sp.**

Fig. 5B

Remarks. A single, small specimen of 1.19 mm length with a squarish outline and a curved posterior rim was recovered, which resembles extant otoliths of *Centrobranchus nigroocellatus* (Günther, 1873) figured in Rivaton & Bourret (1999: pl. 105) and *Centrobranchus andreae* (Lütken, 1892) figured in Ng et al. (2024: figs. 6.2b–3b). However, the inner face of our specimen is eroded, which limits further characterization.

Genus *Dasyscopelus* Günther, 1864

Dasyscopelus obtusirostris (Tåning, 1928)

Fig. 5C

Remarks. Otoliths of *Dasyscopelus* are typically oval to discoid in shape, usually with a finely crenulated ventral margin, in contrast to those of the genus *Diaphus*, which bear pronounced ventral spines. We adopted the taxonomic revision proposed by Martin et al. (2018), who transferred seven species previously classified under the genus *Myctophum* into the valid genus *Dasyscopelus*. In our collection, seven otoliths were assigned to *Dasyscopelus obtusirostris* (Tåning, 1928) based on their more angular outline and more pointed ventral and posterior rims (Rivaton & Bourret 1999: pl. 108, figs. 1–9; Lin & Chang 2012: pl. 10, fig. 78; Ng et al. 2024: fig. 29G). Moreover, five partially eroded specimens were left as *Dasyscopelus* sp.

Genus *Diaphus* Eigenmann & Eigenmann, 1890

Diaphus adenomus Gilbert, 1905

Fig. 6A

Remarks. *Diaphus* otoliths can be distinguished from their relatives by a well-developed rostrum with an excisura, ventral rim denticulation, and a long, clearly divided sulcus (Schwarzhans 2013b). A single specimen in our collection was identified as *Diaphus adenomus* Gilbert, 1905, based on its overall otolith shape, which is characterized by ten fine ventral denticles together with a relatively short, narrow ostium and a convex inner face (Lin & Chang 2012: 10, 78; Schwarzhans 2013b: pl. 12, figs. 6–13).

Diaphus mollis Tåning, 1928

Fig. 6B

Remarks. A single specimen was identified as *Diaphus mollis* Tåning, 1928, based on its compressed otolith shape with a distinct postdorsal depression and a nearly absent excisura (Schwarzhans 2013b: pl. 2, figs. 6–10; Schwarzhans & Ohe 2019, figs. 8L–P). Our specimen also resembles *Diaphus brachycephalus* (Rivaton & Bourret 1999: pl. 112, figs. 1–6; Smale et al. 1995: pl. 17; Schwarzhans 2013b: pl. 5, figs. 1–6), but has fewer ventral rim denticles than *D. brachycephalus*.

Diaphus diademophilus Nafpaktitis, 1978

Fig. 6C

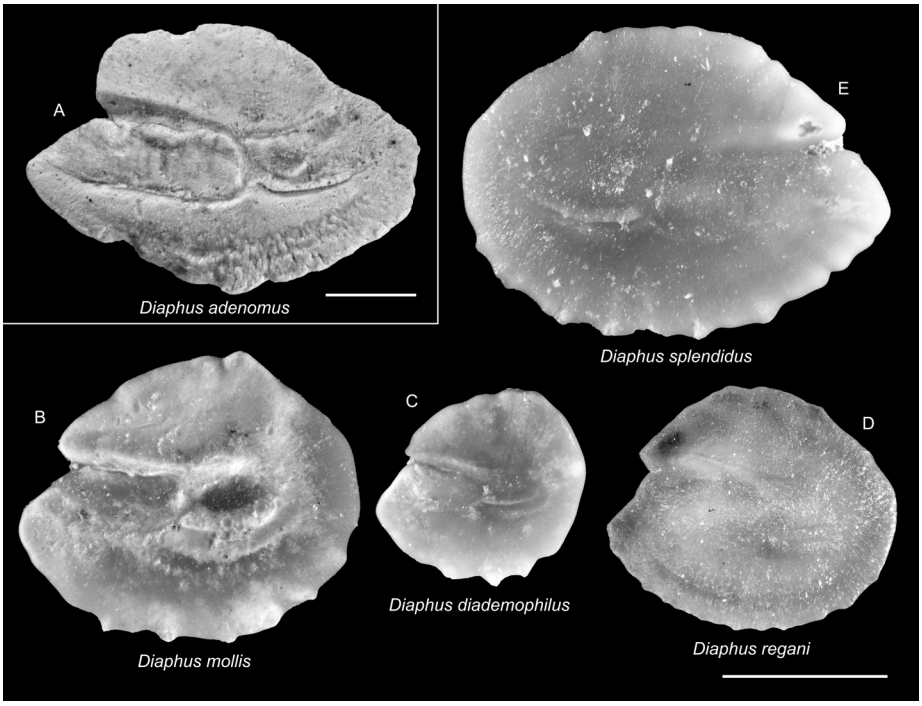

Fig. 6 - Otoliths from Early Pliocene marine sediments in Cabarruyan Island, northwestern Luzon Island, Philippines. Scale bars = 1 mm. Images are inner views unless otherwise indicated. A) *Diaphus adenomus* Gilbert, 1905, NIGSPAL-FISH-033, B) *Diaphus mollis* Tåning, 1928, NIGSPAL-FISH-034, C) *Diaphus diademophilus* Nafpaktitis, 1978, NIGSPAL-FISH-035, D) *Diaphus regani* Tåning, 1932, NIGSPAL-FISH-036, E) *Diaphus splendidus* (Brauer, 1904), NIGSPAL-FISH-037.

Remarks. Three specimens have an otolith similar to that of *Diaphus* but with fewer and more prominent ventral denticles (5–6), a sharper rostrum, and a relatively longer cauda (Schwarzhans 2013b: pl. 5, figs. 9–a2), similar to that of *Diaphus diademophilus* Nafpaktitis, 1978.

Diaphus regani Tåning, 1932

Fig. 6D

2019 *Diaphus regani*—van Hinsbergh & Helwerda, pl. 5, figs. 46–47.

Remarks. A total of 42 specimens in the collection exhibit an overall morphology similar to *Diaphus* and were identified as *Diaphus regani* Tåning, 1932 due to their high ventral denticle count (15–17) and a prominent antero-dorsal elevation (Rivaton & Bourret 1999: pl. 116, figs. 14–20).

Diaphus splendidus (Brauer, 1904)

Fig. 6E

Remarks. *D. splendidus* has a depressed predorsal rim and a well-developed postdorsal angle above the posterior part of the cauda, typically with 9–13 ventral denticles (Lin & Chang 2012: pl. 10, 78). Twenty-nine otoliths were left as *Diaphus* sp. due to poor preservation.

Genus *Diogenichthys* Bolin, 1939

Diogenichthys atlanticus (Tåning, 1928)

Fig. 7A

Remarks. Two otoliths were identified as *Diogenichthys atlanticus*, characterized by small discoid-shaped otoliths with smooth margins and a relatively wide, median-oriented, shallow, and divided sulcus similar to the figured specimen in Rivaton & Bourret (1999: pl. 106, fig. 2) and Schwarzhans & Aguilera (2013: fig. 19a). Our specimen also resembles *Diogenichthys laternatus* (Garman, 1899) figured in Schwarzhans & Aguilera (2013: figs. 21a–b). However, it differs in having a distinctly protruding rostrum, whereas *D. laternatus* has a short rostrum.

Genus *Hygophum* Bolin, 1939

***Hygophum* sp.**

Fig. 7B

Remarks. A single discoid otolith (OL/OH = 1.13) with a wide sulcus positioned near mid-height, blunt rostrum, and a pointed antirostrum resembles *Hygophum macrochir,* similar to the figured specimen in Aguilera & de Aguilera (2001: fig. 11) and Schwarzhans (2013a: pl. 5; figs. 1–2). Most diagnostic features are preserved, although certain por-

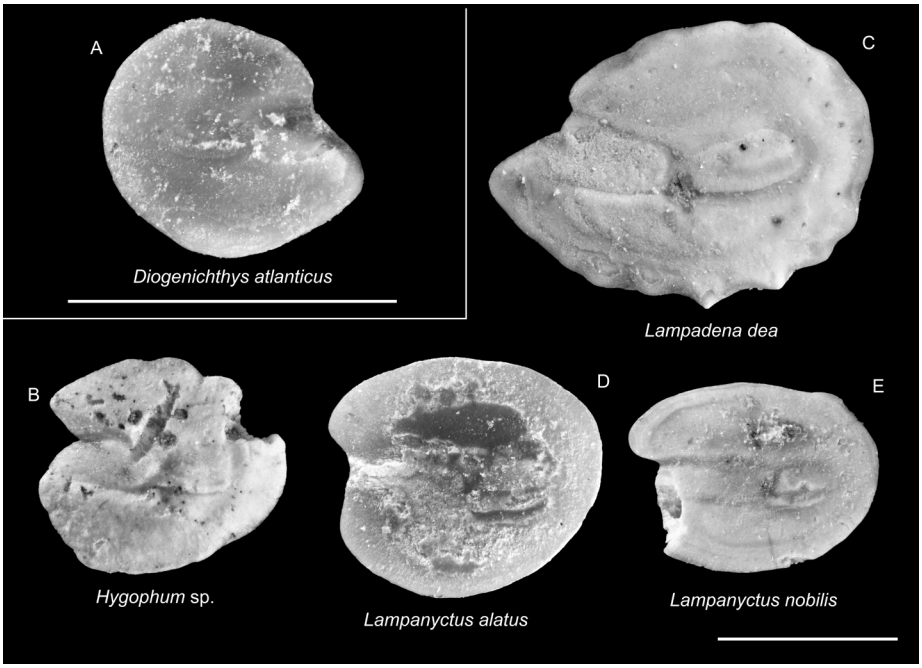

Fig. 7 - Otoliths from Early Pliocene marine sediments in Cabarruyan Island, northwestern Luzon Island, Philippines. Images are inner views unless otherwise indicated. Scale bars = 1 mm. A) *Diogenichthys atlanticus* (Tåning, 1928), NIGSPAL-FISH-039, B) *Hygophum* sp., NIGSPAL-FISH-040, C) *Lampadena dea* Fraser-Brunner, 1949, NIGSPAL-FISH-041, D) *Lampanyctus alatus* Goode & Bean, 1896, NIGSPAL-FISH-043, E) *Lampanyctus nobilis* Tåning, 1928, NIGSPAL-FISH-044.

tions of the specimen are damaged. At present, the specimen is conservatively identified as *Hygophum* sp. pending the availability of additional material.

Genus *Lampadena* Goode & Bean, 1893

Lampadena dea Fraser-Brunner, 1949

Fig. 7C

Remarks. Six spindle-shaped otoliths with ventral denticles were recovered. The rostrum is protruding and pointed, and the antirostrum is short but also pointed, similar to *Lampadena dea* figured in Nafpaktitis & Paxton (1965: fig. 10-6). Although this is uncommon in the collection, all specimens are well preserved, allowing confident identification.

Genus *Lampanyctus* Bonaparte, 1840

Lampanyctus alatus Goode & Bean, 1896

Fig. 7D

2019 *Lampanyctus alatus*—van Hinsbergh & Helwerda, pl. 6, figs. 53–55.
2023 *Lampanyctus alatus*—Lin et al., fig. 9e.

Remarks. A single discoid otolith (OL = 1.52 mm; OH = 1.34 mm; OL/OH = 1.13) closely matches *Lampanyctus alatus* (Smale et al. 1995: pl. 22, fig. D; Rivaton & Bourret 1999: pl. 120, figs. 1–7; Schwarzhans & Ohe 2019: fig. 7L–N).

Lampanyctus nobilis Tåning, 1928

Fig. 7E

2019 *Lampanyctus alatus*—van Hinsbergh & Helwerda, pl. 6, fig. 52.

Remarks. A single *Lampanyctus* otolith with an elongated outline is identified as *Lampanyctus nobilis* (Schwarzhans & Aguilera 2013: pl. 6, fig. 6; Schwarzhans & Ohe 2019: figs. 7R–V). Otoliths of *L. nobilis* typically have an OL/OH ratio of 1.25–1.40 (Schwarzhans & Ohe 2019), but the rostrum of our specimen is broken, preventing a reliable OL/OH measurement. In addition, we recommend the reassignment of the specimen identified as *Lampanyctus alatus* by van Hinsbergh & Helwerda (2019: pl. 6, fig. 52a–b) with OL/OH = 1.3 to *L. nobilis* (see also extant specimen in Fig. S1D, OL/OH = 1.25).

Genus *Lobianchia* Gatti, 1904

Lobianchia dofleini (Zugmayer, 1911)

Fig. 8A

Remarks. Eight discoid-shaped otoliths with an elevated antero-dorsal rim and a broad sulcus are assigned to *Lobianchia dofleini* (Smale et al. 1995: pl. 24, figs. C1–3; Schwarzhans 2013a: pl. 4, figs. 18–20; Schwarzhans 2013b: pl. 15, figs. 1–5). Small otoliths of *L. dofleini* closely resemble the same-sized

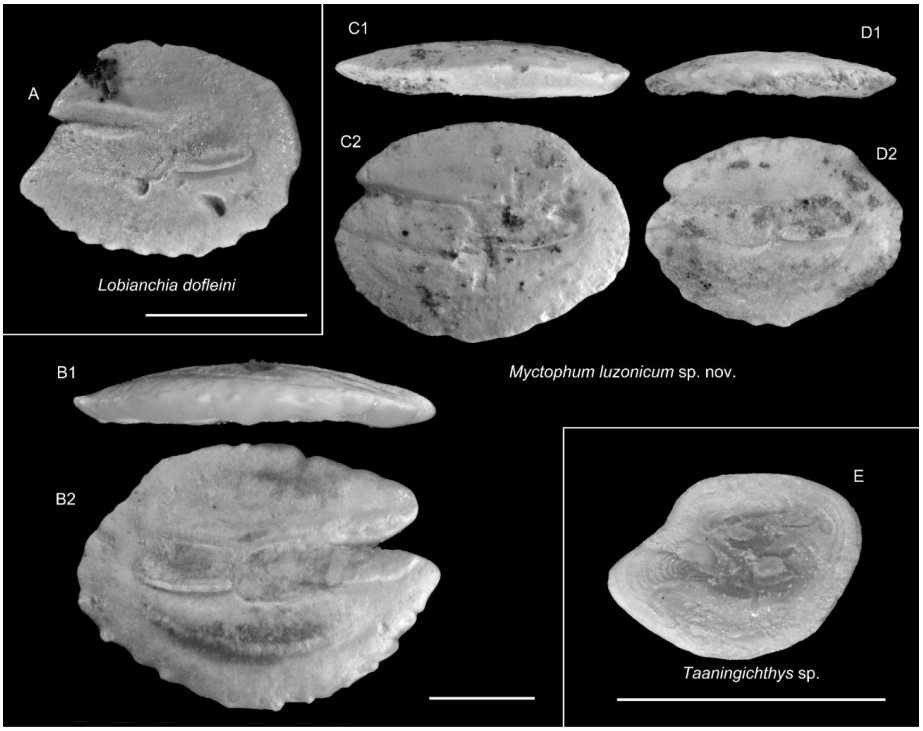

Fig. 8 - Otoliths from Early Pliocene marine sediments in Cabarruyan Island, northwestern Luzon Island, Philippines. Scale bars = 1 mm. Images are inner views unless otherwise indicated. A) *Lobianchia dofleini* (Zugmayer, 1911), NIGSPAL-FISH-046, B–D) *Myctophum luzonicum* sp. nov., B – holotype, NMP-2524, C–D – paratypes, C) NIGSPAL-FISH-015, D) ASIZF0101149, E) *Taaningichthys* sp., NIGSPAL-FISH-048. 1, ventral view; 2, inner view.

Lobianchia gemellarii (Cocco, 1838), but *L. gemellarii* has a narrower sulcus and an antero-dorsal rim that slopes obliquely downward toward the antirostrum (see Lin et al. 2017 for more details). Our specimen also resembles *Diaphus cavallonis* (Brzobohaty and Nolf 2000: pl. 5, figs. 7–14; Lin et al. 2017: figs. 4V–W) but differs in the number of ventral rim denticles. *Diaphus cavallonis* has more than 10 ventral rim denticles (Brzobohaty and Nolf 2000), while our specimen has 9. This matches *L. dofleini*, described as having 6–9 denticles (see Schwarzhans 2013a).

Genus *Myctophum* Rafinesque, 1810

***Myctophum luzonicum* sp. nov.** Mediodia & Lin

Figs. 8B–C

Holotype: NMP-2524 Left sagitta (Fig. 8B), from Cabarruyan Island, Pangasinan, northwestern Luzon Island, Philippines

Paratypes: Two specimens: one specimen NIGSPAL-FISH-015 (Fig. 8C), one specimen ASIZF0101149 (Fig. 8D).

Etymology: The specific name refers to Luzon, the largest island of the Philippines, from which the type material was collected.

Diagnosis: OL/OH = 1.33–1.37, OL/OT = 5.07–5.75, OsL/CaL = 1.18–1.95. Elongated otolith with a straight dorsal rim, steeply angled dorso-posteriorly.

Description. The otolith is discoid to slightly oval in shape, strongly compressed, and has a straight mid-dorsal and gently domed ventral profile (2.45–3.44 mm length). The dorsal rim is arched at the posterior portion with several low and rounded lobes. Ventral rim is more strongly curved and distinctly crenulated along most of its length, with individual crenulations shallow but clearly expressed. Anterior rim bluntly rounded with only a very short, poorly expressed rostral tip in the paratypes, but a clear, pointed rostrum in the holotype. There is an antirostrum and a shallow to deep excisura. Surface of the inner face is otherwise smooth, but corrosion and minor overgrowth occur locally in paratypes, particularly on the dorsal half of the otolith (Fig. 8C–D). The sulcus is long, narrow, and supramedian, extending over approximately two-thirds of the otolith's length. The sulcus is slightly inclined anterodorsally. Ostium anterior, rectangular-oval, shallow with a flat to gently concave floor, and only moderately wider and longer than the cauda (OsL/CaL = 1.18–1.95). Cauda is distinctly narrower, more tubular, slightly deeper than the ostium, and nearly straight, terminating before the posterior rim. The outer face is convex with no distinct umbo.

Remarks. *Myctophum luzonicum* differs from these discoid congeners in several consistent features including a slightly more elongate outline (OL/OH > 1.3), a more strongly crenulated ventral rim with deeper and more widely spaced denticles, a conspicuously deep, continuous ventral furrow, and a sulcus in which the ostium is only moderately longer than the cauda, rather than being more than

twice as long as the cauda, as described for several other *Myctophum* species. Compared with its congeners, *M. luzonicum* differs from *M. aurolaternatum* Garman, 1899 (Rivaton & Bourret 1999: pl. 107, figs. 12–13) in its more discoid shape and longer cauda and from *M. nitidulum* Garman, 1899 (Rivaton & Bourret 1999: pl. 107, figs. 17–22) in its elongated overall shape, more flattened dorsal margin, and elongated cauda. These characters, together with the metric ranges provided above, support recognition of *M. luzonicum* as a distinct species. There are three non-type specimens in the collection (NIGSPAL-FISH-047).

Occurrence. Currently known only from Cabarruyan Island, Pangasinan, northwestern Luzon Island, Philippines.

Genus *Taaningichthys* Bolin, 1959

***Taaningichthys* sp.**

Fig. 8E

Remarks. Two discoid otoliths with slightly flattened dorsal margins and convex ventral margins arched upward toward the posterior region were recovered. The sulcus is slightly eroded but wide and median-oriented, with a distinctly separated, dorsally raised ostium and cauda. The overall morphology of our specimen closely resembles that of *Taaningichthys bathyphilus* (Rivaton & Bourret 1999: pl. 124, figs. 1–5). However, due to poor preservation, we conservatively assign it to *Taaningichthys* sp.

Order **Gadiformes** Goodrich, 1909
Family Macrouridae Bonaparte, 1831
Genus *Coelorinchus* Giorna, 1809

***Coelorinchus* sp.**

Fig. 9A

Remarks. Two thick, oblong otoliths with crenulated margins and an angled postero-ventral rim were recovered. They closely resemble *Coelorinchus* cf. *australis* figured in van Hinsbergh & Helwerda (2019: figs. 65–67). However, the specimens are abraded and have damaged margins, so we conservatively assign them to *Coelorinchus* sp.

Genus *Hymenocephalus* Giglioli, 1884

Hymenocephalus cf. iwamotoi

Fig. 9B

Remarks. Otoliths of *Hymenocephalus* can be characterized based on the presence of a well-developed predorsal lobe and sulcus with equal lengths of the ostium and cauda (Schwarzhans 2014). Four high-bodied otoliths with a well-developed, massive predorsal lobe, an anteriorly inclined lobe, and a straight, deep, clearly separated sulcus closely resemble those of *Hymenocephalus iwamotoi* Schwarzhans 2014 (Schwarzhans 2014, fig. 11F–H). Our specimen is more compact than the elongated *Hymenocephalus longibarbis* (Günther, 1887) (Schwarzhans 2014: figs. 8D–L). Modern specimens of *H. iwamotoi* are only known from off Browse Island, Western Australia, and are likely endemic to that region. Based on these observations, we identified our specimen as *H.* cf. *iwamotoi*, pending the collection of additional well-preserved specimens.

Hymenocephalus torvus Smith & Radcliffe, 1912

Fig. 9C

Remarks. Twenty-four otoliths were identified as *H. torvus* based on their large dorsal rim, a rounded posterior tip, and a non-divided sulcus (Schwarzhans 2014: figs. 33C–G). The difference between *H. torvus* and *H. aeger* can be distinguished primarily by the OL/OH ratio (*H. torvus* OL/OH = 0.8–0.9; *H. aeger* OL/OH = 0.9–1.0: Schwarzhans 2014). Our specimens have OL/OH = 0.802–0.907, which are more compact than those of *H. aeger*.

Genus *Hymenogadus* Gilbert & Hubbs, 1920

Hymenogadus gracilis (Gilbert & Hubbs, 1920)

Fig. 9D

Remarks. Fourteen moderately elongated otoliths exhibiting a prominent dorsal extension from the middle to the anterior region and a straight, narrow sulcus were recovered. These specimens closely resemble *Hymenogadus gracilis* (Gilbert & Hubbs, 1920) figured in Schwarzhans (2014: figs. 6E–I). Although Macrouridae are dominant within the assemblage, *H. gracilis* is the only macrourid species identified at Site 3. Additionally, 21 specimens were assigned to *Hymenocephalus* sp. due to insufficient preservation of diagnostic features for species-level identification.

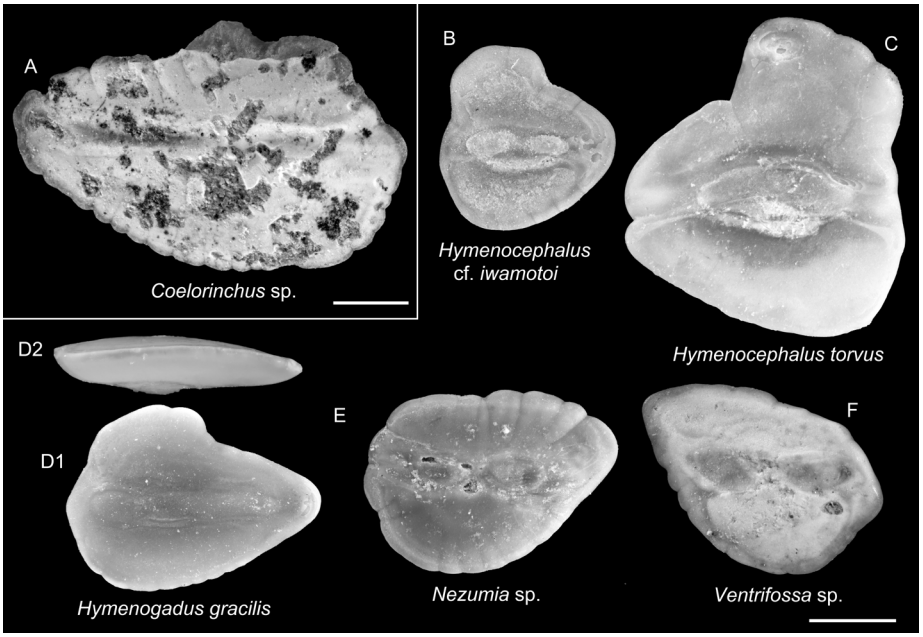

Fig. 9 - Otoliths from Early Pliocene marine sediments in Cabarruyan Island, northwestern Luzon Island, Philippines. Scale bars = 1 mm. Images are inner views unless otherwise indicated. A) *Coelorinchus* sp., NIGSPAL-FISH-050, B) *Hymenocephalus* cf. *iwamotoi*, NIGSPAL-FISH-051, C) *Hymenocephalus torvus* Smith & Radcliffe, 1912, NIGSPAL-FISH-053, D) *Hymenogadus gracilis* (Gilbert & Hubbs, 1920), NIGSPAL-FISH-054, E) *Nezumia* sp., NIGSPAL-FISH-055, F) *Ventrifossa* sp., NIGSPAL-FISH-056.

Genus *Nezumia* Jordan, 1904

***Nezumia* sp.**

Fig. 9E

Remarks. Three otoliths have a rhomboidal outline, with a posterior margin that is dorsally angled and an anterior margin that is rounded. Sulcus is straight and narrow with a wall-like collum. Our specimen resembles *Nezumia ornata* (Bassoli, 1906), as figured in Lin et al. (2015, fig. 8K). However, we leave the identification to *Nezumia* sp. Additional fossil material and comparative extant otoliths are required to enable more precise taxonomic identification.

Genus *Ventrifossa* Gilbert & Hubbs, 1920

***Ventrifossa* sp.**

Fig. 9F

Remarks. A single otolith was assigned to *Ventrifossa* sp. based on its thick, rhomboidal outline with lobulated margins and a straight and divided sulcus. It shows similarities to *Ventrifossa rhipidodorsalis* Okamura, 1984 (Lin & Chang 2012: pl. 12, 80) and *Ventrifossa longibarbata* Okamura, 1982 (Lin & Chang 2012: pl. 12, 80; Ng et al. 2024: fig. 38B) but differs by its straighter dorsal rim and a distinctly triangular postero-dorsal rim. However, because only a single specimen is available, we conservatively retain the identification at the genus level.

Family Bregmacerotidae Gill, 1872

Genus *Bregmaceros* Thompson, 1840

***Bregmaceros japonicus* Tanaka, 1908**

Fig. 10A

2019 *Bregmaceros* cf. *mcclellandi*—van Hinsbergh & Helwerda, pl. 7, fig. 63.
2023 *Bregmaceros japonicus*—Lin et al., figs. 11b–d.

Remarks. There are 109 thin specimens in our collection that resemble the extant *Bregmaceros* otolith based on the overall shape and a solid bridge collum that separates ostium and cauda (Lin & Chang 2012). Fifty-two otoliths with a wide and extended posterior lobe behind the caudal depression were identified as *Bregmaceros japonicus* Tanaka, 1908 (Lin & Chang 2012: pl. 11, fig. 79; Ng et al. 2024: fig. 40F).

***Bregmaceros nectabanus* Whitley, 1941**

Fig. 10B

2019 *Bregmaceros* cf. *mcclellandi*—van Hinsbergh & Helwerda, pl. 7, figs. 61–62, 64.
2023 *Bregmaceros nectabanus*—Lin et al., figs. 11j–k.

Remarks. A total of twenty-nine otoliths were identified as *Bregmaceros nectabanus* Whitley, 1941 (Lin & Chang 2012: pl. 11, 79) due to their less pronounced posterior lobe located above the caudal depression. Additionally, 28 otoliths are classified as *Bregmaceros* sp. due to partial erosion, which limits our ability to identify them to the species level.

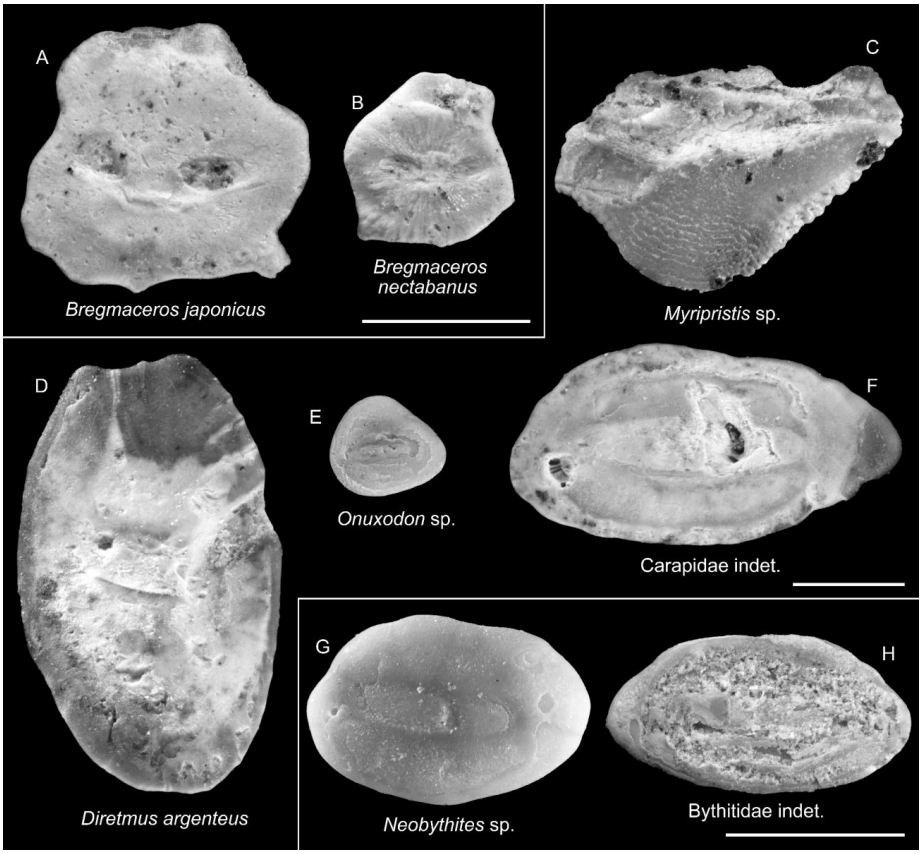

Fig. 10 - Otoliths from Early Pliocene marine sediments in Cabarruyan Island, northwestern Luzon Island, Philippines. Scale bars = 1 mm. Images are inner views unless otherwise indicated. A) *Bregmaceros japonicus* Tanaka, 1908, NIGSPAL-FISH-057, B) *Bregmaceros nectabanus* Whitley, 1941, NIGSPAL-FISH-058, C) *Myripristis* sp., NIGSPAL-FISH-060, D) *Diretmus argenteus* Johnson, 1864, NIGSPAL-FISH-061, E) *Onuxodon* sp., NIGSPAL-FISH-062, F) Carapidae indet., NIGSPAL-FISH-063, G) *Neobythites* sp., NIGSPAL-FISH-064, H) Bythitidae indet., NIGSPAL-FISH-065.

Order **Beryciformes** Regan, 1909
Family Holocentridae Bonaparte, 1833
Genus *Myripristis* Cuvier, 1829

***Myripristis* sp.**

Fig. 10C

Remarks. A single heart-shaped otolith, with a straight dorsal rim longer than the curved ventral rim, was recovered. The sulcus is deep and positioned near the dorsal rim, with an oval ostium reaching the anterior rim and a straight cauda. The specimen resembles the otoliths of extant species *Myripristis greenfieldi* Randall & Yamakawa, 1996 and *Myripristis pralinia* Cuvier, 1829, both of which are figured in Lin & Chang (2012: pl. 18, 86). However, the otolith is partially damaged, particularly along the dorsal region.

Order **Trachichthyiformes** Moore, 1993
Family Diretmidae Gill, 1893
Genus *Diretmus* Johnson, 1864

***Diretmus argenteus* Johnson, 1864**

Fig. 10D

Remarks. A specimen was identified as *Diretmus argenteus* because of its tall-shaped otolith (OL/OH = 0.60) with flat dorsal and U-shaped ventral rims identical to the figured specimen in Lin & Chang (2012: pl. 17, 85) and Ng et al. (2024: fig. 40G). Although the inner face is poorly preserved, a long, slightly upturned sulcus is visible, with a flared ostium and an elongate cauda that support our identification.

Order **Ophidiiformes** Berg, 1937
Family Carapidae Poey, 1867
Genus *Onuxodon* Smith, 1955

***Onuxodon* sp.**

Fig. 10E

2023 *Onuxodon* sp.—Lin et al., figs. 11e–f.

Remarks. A single triangular otolith (OL/OH = 1.16) has a smooth dorsal rim and a flat inner face. The sulcus is straight and median-oriented with a fused colliculum. Our specimen is small and has a comparatively short posterior region, consistent with the genus *Onuxodon* (Lin et al. 2023). It resembles *Onuxodon margaritiferae* (Rendahl, 1921)

as figured by Rivaton & Bourret (1999: pl. 9, figs. 7–8), but differs in having a more slender anterior rim. However, marginal abrasion obscures diagnostic features, so we conservatively identify the specimen as *Onuxodon* sp. The Carapidae indet. otolith figured by van Hinsbergh & Helwerda (2019: pl. 7, fig. 70) is similar to our specimen. However, the published image lacks sufficient detail for a conclusive comparison, so we do not base a definitive identification on it alone. In addition, one otolith in our collection was assigned to Carapidae indet. based on the overall outline and sulcus position (Fig. 10f).

Family Ophidiidae Rafinesque, 1810
Genus *Neobythites* Goode & Bean, 1885

***Neobythites* sp.**
Fig. 10G

2019 *Neobythites* sp.—van Hinsbergh & Helwerda, pl. 7, fig. 7.
2023 *Neobythites* sp.—Lin et al., figs. 13a–b.

Remarks. Three specimens were identified as *Neobythites* sp. based on their oblong-shaped otoliths, median and divided sulcus, and a blunt and short rostrum. The specimens resemble *Neobythites japonicus* (Su et al. 2023: fig. 2) and *Neobythites stigmosus* (Lin & Chang 2012: pl. 81). However, the otoliths in our collection are juvenile. Better-preserved materials are needed to refine identification within *Neobythites*.

Family Bythitidae Gill, 1861
Bythitidae indet.
Fig. 10H

2023 Bythitidae indet.—Lin et al., figs. 13c1–2.

Remarks. A single otolith was assigned to Bythitidae. It has an elongated, almost spindle-like, otolith (OL/OH = 1.93) with moderate thickness and tapering ends. The dorsal and ventral margins are smooth, almost symmetrically arched. The anterior and posterior rims are broadly rounded. However, the inner face of our specimen is heavily abraded. We can only see a very broad, low median depression that hints at the position of the sulcus, while the ostium and cauda are not distinguishable. Accordingly, we restrict identification to the family level until additional specimens are available.

Order **Kurtiformes** Jordan, 1923
Family Apogonidae Günther, 1859
Apogonidae indet.
Figs. 11A–B

?2019 *Apogon* sp.—van Hinsbergh & Helwerda, pl. 8, figs. 77–79, 81.

Remarks. Thirty-six elliptic otoliths show a deep, median, clearly divided sulcus with an oblong ostium, an elongate straight cauda, and a prominent dorsal depression consistent with the figured specimens in Smale et al. (1995: pl. 67, figs. A–D) and Chew et al. (2025: figs. 4a–b). Two morphotypes are recognized in our material: Morphotype A shows a straight ventral rim, blunt posterior rim, and a straight cauda (Fig. 10A), whereas Morphotype B has a curved ventral rim and an extended posterior rim (Fig. 10B). Four specimens in van Hinsbergh & Helwerda (2019: pl. 8, figs. 77–79, 81) resembles morphotype A in our collection. However, given that most of the otoliths are juvenile, we conservatively identify them as Apogonidae indet. until new fossil otoliths are recovered.

Order **Gobiiformes** Günther, 1880
Family Gobiidae Cuvier, 1816
Genus *Gobiopterus* Bleeker, 1874

***Gobiopterus* sp.**
Figs. 11C–D

2019 Gobiidae indeterminate—van Hinsbergh & Helwerda, pl. 8, figs. 90a–b.

Remarks. Six circular otoliths characterized by a nearly flat inner face and a narrow but deep arrow-shaped sulcus are assigned to *Gobiopterus*. Our specimen resembles *Gobiopterus semivestitus* (Munro, 1949) figured in Schwarzhans (2019: fig. 112, 16–17) and those figured by van Hinsbergh & Helwerda (2019: pl. 8, figs. 90a–b) as Gobiidae indet. Due to the difficulty of species-level identification for most gobiid otoliths, we conservatively retain our specimens as *Gobiopterus* sp.

Genus *Priolepis* Valenciennes, 1837

***Priolepis* sp.**
Fig. 11E

2019 *Priolepis* sp.—van Hinsbergh & Helwerda, pl. 8, fig. 9.

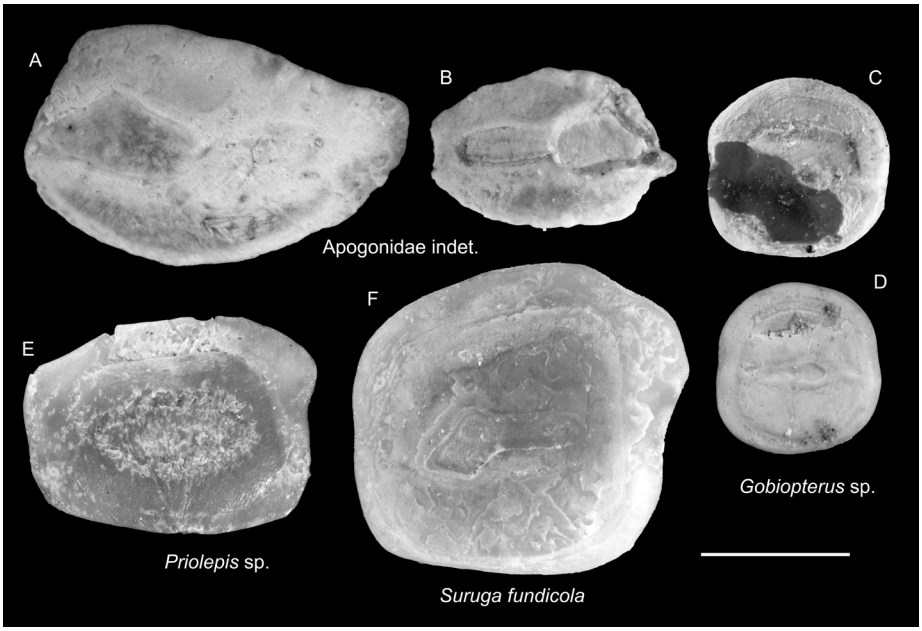

Fig. 11 - Otoliths from Early Pliocene marine sediments in Cabarruyan Island, northwestern Luzon Island, Philippines. Scale bar = 1 mm. Images are inner views unless otherwise indicated. A–B) Apogonidae indet., NIGSPAL-FISH-066, C–D) *Gobiopterus* sp., NIGSPAL-FISH-067, E) *Priolepis* sp., NIGSPAL-FISH-068, F) *Suruga fundicola* Jordan & Snyder, 1901, NIGSPAL-FISH-069.

Remarks. A thick, rectangular gobiid otolith (OL/OH = 1.36) is assigned to *Priolepis* sp. The overall morphology matches the *Priolepis* sp. otolith reported by van Hinsbergh & Helwerda (2019: pl. 8, fig. 91), suggesting a single morphotype in the assemblage; it also matches several specimens figured by Schwarzhans et al. (2020: pl. 8, figs. 2–9) and Lin et al. (2023; figs. 14a–d). However, the inner face of our sample is slightly damaged, and only one specimen is available, which limits the ability to make a species-level diagnosis.

Genus *Suruga* Jordan & Snyder, 1901

Suruga fundicola Jordan & Snyder, 1901
Fig. 11F

2019 *Suruga fundicola*—van Hinsbergh & Helwerda, pl. 8, figs. 84–88.

Remarks. Three specimens with thick, square-shaped gobiid otoliths were identified as *Suruga fundicola*. The sulcus is short, median, and deeply incised, similar to the figured specimen *S. fundicola* in Ohe (1983: pl. 10, figs. 1–4) and *Suruga* aff. *fundicola* in Lin et al (2023: fig. 14g).

Order **Atheriniformes** Rosen, 1964
Family Atherinidae Risso, 1827
Genus *Atherinomorus* Fowler, 1903

Atherinomorus lacunosus (Forster, 1801)
Fig. 12A

Remarks. A single circular (OL/OH = 1.01) otolith with concave inner face and convex outer face, with deep and supramedian sulcus, was identified as *Atherinomorus lacunosus* (Smale et al. 1995, pl. 39, fig. B1–3; Lin & Chang 2012: pl. 15, 83). Despite damage to the anterior region of our specimen, the funnel-like ostium and the narrow, elongate cauda, which curves ventrally toward the posterior end, are well preserved and support a species-level identification.

Order **Beloniformes** Berg, 1940
Family Belonidae Bonaparte, 1835

Belonidae indet.
Fig. 12B

Remarks. A single juvenile otolith is referred to Belonidae based on its oblong outline tapering to a pointed anterior rim and a straight, median sulcus with an open ostium and an elongate cauda, matching figured belonid otoliths (Rivaton & Bourret 1999: pl. 10:17–20, 11:1–9; Nolf 2013: pl. 156). However, the inner face is poorly preserved, so the identification is conservatively restricted to the family level.

Order **Carangiformes** Patterson, 1993
Family Carangidae Rafinesque, 1815
Genus *Decapterus* Bleeker, 1851

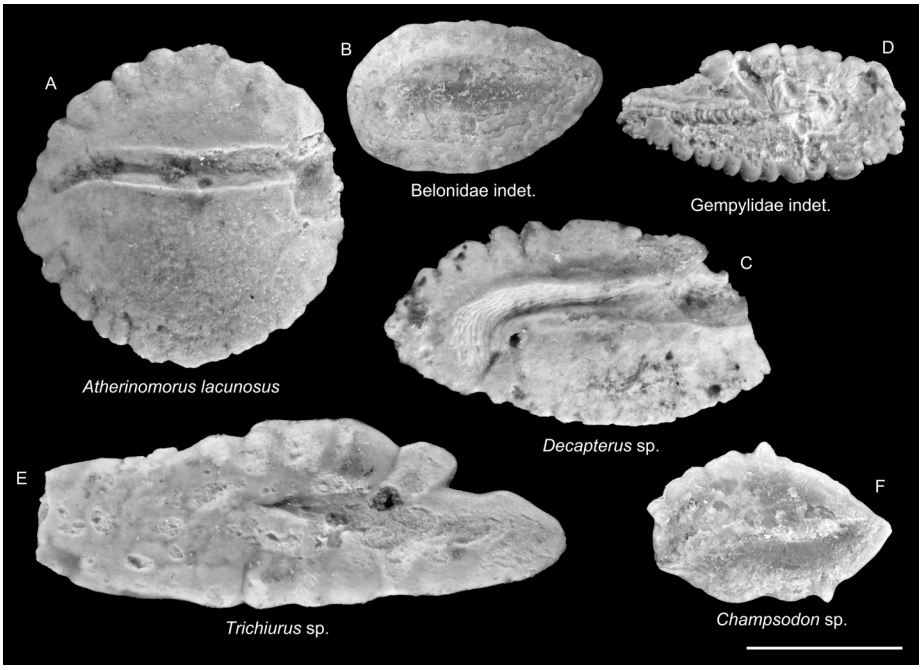

Fig. 12 - Otoliths from Early Pliocene marine sediments in Cabarruyan Island, northwestern Luzon Island, Philippines. Scale bar = 1 mm. Images are inner views unless otherwise indicated. A) *Atherinomorus lacunosus* (Forster, 1801), NIGSPAL-FISH-071, B) Belonidae indet., NIGSPAL-FISH-072, C) *Decapterus* sp., NIGSPAL-FISH-073, D) Gempylidae indet. NIGSPAL-FISH-074, E) *Trichiurus* sp., NIGSPAL-FISH-075, F) *Champsodon* sp., NIGSPAL-FISH-076.

***Decapterus* sp.**

Fig. 12C

?2019 Carangidae indet.—van Hinsbergh & Helwerda, pl. 8, figs. 92a–b.

Remarks. A single spindle-like otolith with a crenate margin, concave outer face, and deep and narrow sulcus was assigned to *Decapterus* sp. (Smale et al. 1995: pl. 72, figs. A–C) and Lin and Chang (2012: pl. 33, 101). Our specimen also resembles the otolith figured by van Hinsbergh & Helwerda (2019: pl. 8, figs. 92a–b) as Carangidae indet. However, because only a single, anteriorly broken specimen is available, a species-level assignment is not possible.

Order **Scombriformes** sensu Davis et al., 2016
Family Gempylidae Gill, 1862

Gempylidae indet.

Fig. 12D

2019 Gempylidae sp. 1—van Hinsbergh & Helwerda, pl. 8, figs. 75–76.

Remarks. Two juvenile otoliths with pyriform shape, lobed margins, pointed anterior rim, and blunt posterior rim resemble those of *Promethichthys prometheus* (Cuvier, 1832) (Lin et al. 2015: fig. 7:1; Fig. S1g). Our specimen is heavily eroded, which makes it difficult to identify. For this reason, we classify it as Gempylidae indet. Notably, two otoliths identified as Gempylidae sp. 1 by van Hinsbergh and Helwerda (2019: pl. 8, figs. 75–76) also resemble *P. prometheus* (Fig. S1D).

Family Trichiuridae Rafinesque, 1810
Genus *Trichiurus* Linnaeus, 1758

***Trichiurus* sp.**

Fig. 12E

Remarks. A single spindle-shaped otolith with a flat inner face and a dorso-ventrally concave outer face was recovered. The sulcus is short, deep, and undivided, which widens anteriorly and tapers posteriorly. It closely resembles those of *Trichiurus lepturus* Linnaeus, 1758 (Lin & Chang 2012: pl. 61, 129). However, because the inner face is poorly preserved, we conservatively assign it to *Trichiurus* sp.

Order **Acropomatiformes** *sensu* Davis et al., 2016
Family Champsodontidae Jordan & Snyder, 1902
Genus *Champsodon* Günther, 1867

***Champsodon* sp.**

Fig. 12F

2023 *Champsodon* sp.—Lin et al., fig. 15h.

Remarks. Two pentagonal otoliths with a pointed anterior rim (posterior rim damaged in

our specimen) and a highly angled mediodorsal rim are recovered. The sulcus shows an oblong ostium and a narrow cauda that flexes downward toward the postero-ventral rim. Our specimen resembles *Champsodon guentheri* Regan, 1908 (Rivaton & Bourret 1999: pl. 153, figs. 1–4). However, because species-level identification based solely on otoliths is often challenging in this family (Schwarzhans 2019), we conservatively assign the specimen to *Champsodon* sp.

Family Acropomatidae Gill, 1893
Genus *Parascombrops* Alcock, 1889

Parascombrops schwarzhansi van Hinsbergh & Helwerda, 2019
Fig. 13A

2019 *Parascombrops schwarzhansi*—van Hinsbergh & Helwerda, pl. 10, figs. 102–107.

Remarks. Eight fusiform otoliths with general morphological features identical to the genus *Parascombrops* (Schwarzhans & Prokofiev 2017) were recovered in our sample. The pronounced crenulation of the dorsal and ventral margins in our specimen was used to identify it as *Parascombrops schwarzhansi* (see van Hinsbergh & Helwerda 2019, for a full description).

***Parascombrops* sp.**
Fig. 13B

Remarks. Three *Parascombrops* otoliths with a more compact outline (OL/OH = 1.6) were recovered, compared with *P. schwarzhansi* (OL/OH = 1.7 – 1.9). Our specimen resembles *Parascombrops* aff. *serrotospinosus* (van Hinsbergh & Helwerda 2019: pl. 9, fig. 101) but differs in having a more rounded posterior rim and a weakly developed antirostrum. Given that we have only three otoliths in our collection, we conservatively assign the specimens to *Parascombrops* sp.

Order **Perciformes** sensu Davis et al., 2016
Family Leiognathidae Gill, 1893
Genus *Equulites* Fowler, 1904

***Equulites* sp.**
Fig. 13C

Remarks. A single, oval otolith (OL = 1.68 mm; OH = 1.29 mm; OL/OH = 1.30) with lobed margins was recovered. The sulcus is wide and deep, with a flared ostium and a short, narrow cauda. Our specimen resembles *Equulites leuciscus* (Günther, 1860) (Lin & Chang 2012: pl. 34, 102). However, because the single specimen is juvenile and poorly preserved, we conservatively identify it as *Equulites* sp.

Family Cepolidae Rafinesque, 1815
Cepolidae indet.
Fig. 13D

Remarks. Two otoliths with oval ostium that slightly flexes upward and a sac-like cauda resemble those of *Acanthocepola indica* (Day, 1888) (Lin & Chang 2012: pl. 47, 115). However, because the specimens are juvenile, diagnostic characters are not discernible, and we conservatively assign them to Cepolidae indet.

Family Triglidae Rafinesque, 1815
Genus *Satyrichthys* Kaup, 1873

***Satyrichthys* sp.**
Fig. 13E

Remarks. Two triangular *Satyrichthys* otoliths with slightly pointed posterior rim and shallow sulcus that bears oval collicula were recovered. The general morphology resembles *Satyrichthys rieffeli* (Kaup, 1859) (Lin & Chang 2012: pl. 24, 92). However, we conservatively identify it as *Satyrichthys* sp., as some parts are worn and eroded.

Order **Scorpaeniformes** Garman, 1899
Scorpaeniformes indet.
Fig. 13F

Remarks. Three thick, spindle-shaped otoliths with smooth margins and a short but well-defined sulcus were identified as scorpaeniform otoliths. The inner faces of our specimens are poorly preserved, making a detailed description of the sulcus difficult. Our spindle-shaped otoliths resembles the families Bembridae (Lin & Chang 2012: pl. 24, 92), Platycephalidae (Lin & Chang 2012: pl. 24, 92) and Scorpaenidae (Smale et al. 1995: pl. 48, figs. D–G, pl. 49, figs. A–L, pl. 50, figs. A–H, pl. 51, figs.

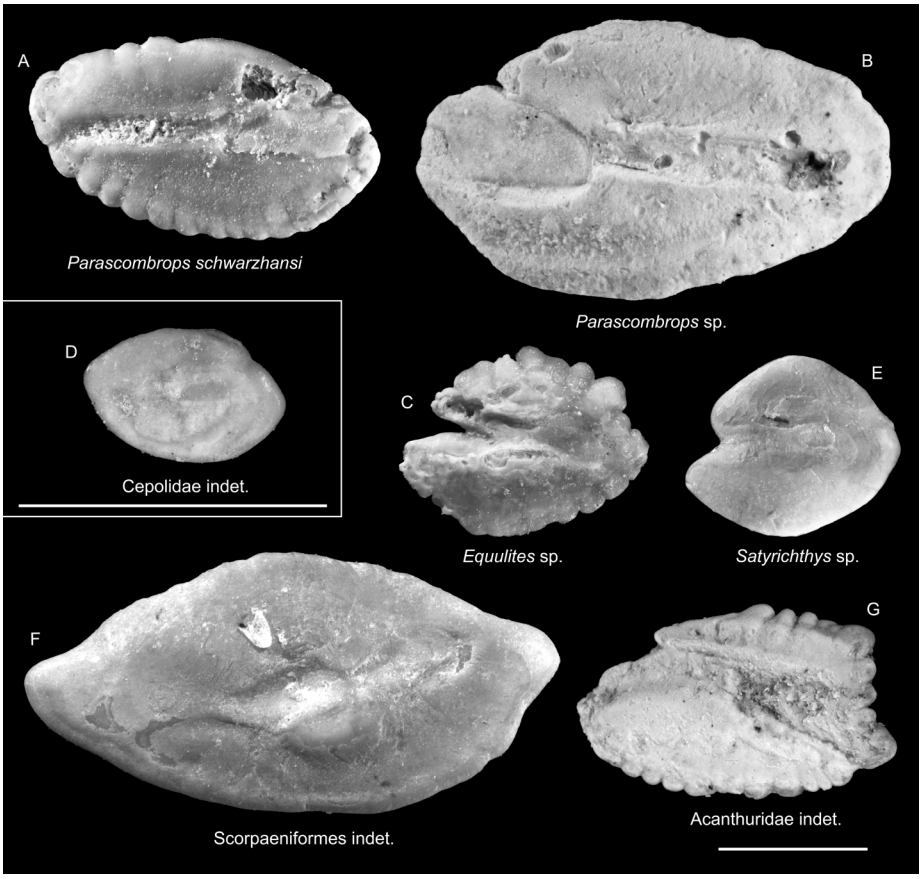

Fig. 13 - Otoliths from Early Pliocene marine sediments in Cabarruyan Island, northwestern Luzon Island, Philippines. Images are inner views unless otherwise indicated. Scale bars = 1 mm. A) *Parascombrops schwarzhansi* van Hinsbergh & Helwerda, 2019, NIGSPAL-FISH-077, B) *Parascombrops* sp., NIGSPAL-FISH-078, C) *Equulites* sp., NIGSPAL-FISH-079, D) Cepolidae indet., NIGSPAL-FISH-080, E) *Satyrichthys* sp., NIGSPAL-FISH-081, F) Scorpaeniformes indet., NIGSPAL-FISH-082, G) Acanthuridae indet., NIGSPAL-FISH-083.

A–D) than the more compact otoliths of Aploactinidae (Lin & Chang 2012: pl. 22, 90), Dactylopteridae (Lin & Chang 2012: pl. 20, 88), Hoplichthyidae (Lin & Chang 2012: pl. 25, 93), Peristediidae (Lin & Chang 2012: pl. 23, 91), and Triglidae (Smale et al. 1995: pl 52, figs. B–5, pl. 53, figs. A–E; Lin & Chang 2012: pl. 23, 91). The overall shape and the short sulcus resemble the otoliths of the genus *Trachyscorpia* Ginsburg, 1953 (Smale et al. 1995: pl. 51, fig. A) compared to the elongated sulcus of Bembridae (Lin & Chang 2012: pl. 24, 92) and Platycephalidae (Lin & Chang 2012: pl. 24, 92). However, due to poor specimen preservation, we conservatively assign them to Scorpaeniformes indet., pending the collection of better-preserved material.

Order **Acanthuriformes** Jordan, 1923
Family Acanthuridae Bonaparte, 1835
Acanthuridae indet.
Fig. 13G

Remarks. Two otoliths with convex inner face and concave outer face, marked postero-dorsal angle, and truncated posterior rim exhibit features of acanthurid otoliths. Our specimen further resembles those of *Acanthurus* or *Naso* (Smale et al. 1995: pl. 130, fig. D4; Lin & Chang 2012: pl. 59, 127), but due to limited preservation, we restrict identification to the family level.

Otolith density, sample coverage, and diversity indices

A total of 1,225 otoliths were recovered from 29 bulk sediment samples (Tab. 1). Of these, 127 specimens were retained as indeterminate due to incomplete preservation or insufficient diagnostic characters, and five were utricular otoliths (Tab. 1). The remaining 1,093 sagittae were identified to 69 taxa representing 28 families. Mean otolith density across all samples was 14 otoliths kg^{-1} (Tab. S1).

Family-level rank abundance patterns (based on the 1,093 identified sagittae) indicate strong dominance by Myctophidae (n = 527) and Sternoptychidae (n = 291), followed by Bregmacerotidae (n = 109), Macrouridae (n = 69) and Apogonidae (n = 36), reflecting a community structured around a small number of abundant families with a long tail of less common taxa (Fig. 14). Rarefaction/extrapolation curves for q = 0 (^0D) shows a continued upward trajectory, indicating incomplete sampling

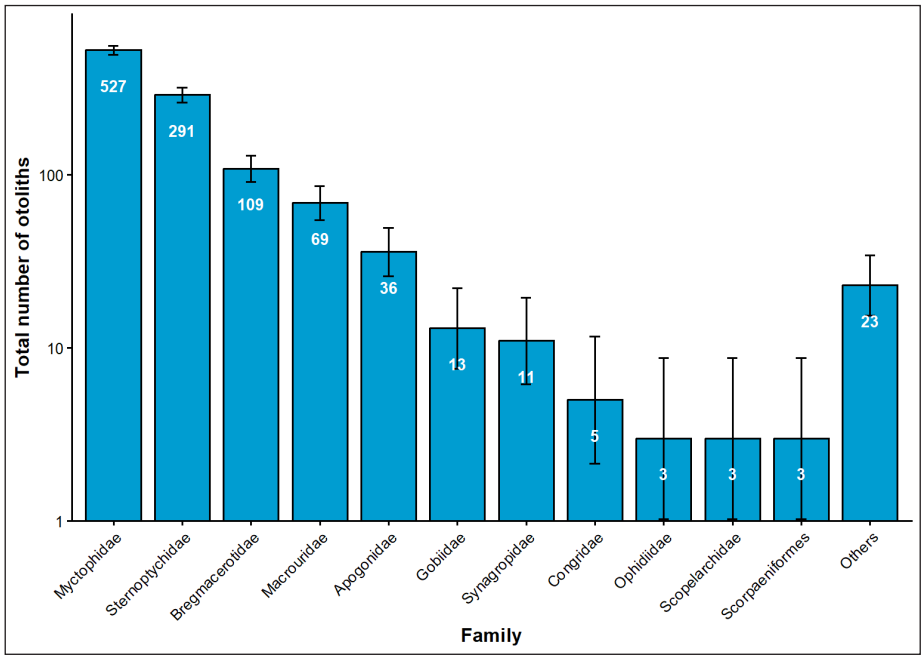

Fig. 14 - Rank abundance of otolith order/families from Early Pliocene marine sediments in Cabarruyan Island, northwestern Luzon Island, Philippines. Families are ranked by total abundance and plotted on a log scale. Families represented by fewer than three specimens were combined and reported under Others, and indeterminate specimens and non-saccular otoliths were not included. Numbers inside the bars indicate total specimen counts. Binomial 95% confidence intervals were calculated using Wilson's method and represent uncertainty in abundance estimates relative to the total sample size.

of rare taxa and suggesting richness could approach ~90 taxa with additional sampling (Fig. 15). In contrast, diversity estimates that emphasize abundant (q = 1; ^1D) and dominant (q = 2; ^2D) taxa reach asymptotes (Fig. 15), indicating sufficient sampling for common and dominant elements of the assemblage (Fig. 15). Coverage-standardized Hill numbers indicate an effective diversity of ~15 common taxa (^1D = 14.93 ± 0.64) and ~7 dominant taxa (^2D = 7.23 ± 0.3) (Tab. S3). Otolith density differs significantly among sites, with Site 1 higher than Sites 2 and 3 (p < 0.05, Kruskal–Wallis with Dunn's post hoc tests; Fig. 15).

Discussion

Taxonomic notes on van Hinsbergh & Helwerda (2019)

We provide an updated taxonomic note on the identifications reported by van Hinsbergh & Helwerda (2019) (see Tab. 1). Specifically, we propose the following revisions.

1. We reassess material previously compared with *Lampanyctus alatus* (pl. 6, figs. 52, 54–55). The specimen in pl. 6, fig. 52 has a pronounced antirostrum that closely matches that of *Lampanyctus nobilis* Tåning, 1928 (see Fig. 7E and the extant counterpart in Fig. S1E). In contrast, two specimens in pl. 6, figs. 54–55 exhibit rostrum and antirostrum of comparable size, a configuration more consistent with *Lampanyctus tenuiformis* (Brauer, 1906) (see Smale et al. 1995: pl. 23, figs. G1–2 and Fig. S1F).

2. The two specimens treated as "Apogonidae indeterminate" (pl. 8, figs. 82a–83b) can be reassigned to *Xeniamia atrithorax* Fraser & Prokofiev, 2016 based on overall morphology (Fraser & Prokofiev 2016: figs. 8A–D and Fig. S1G).

3. The specimens listed as Gobiidae indet. (pl. 8, figs. 90a–b), can be referred to *Gobiopterus* sp. (see above, remarks under the taxon).

4. The specimen figured as "Sparidae indeterminate" (pl. 9, Fig. 93) is unlikely to be a sparid; its otolith morphology is more consistent with juveniles of *Malakichthys* Döderlein, 1883 (see figs. 16e–g in Lin et al. 2023; Fig. S1H–I).

5. We also updated several names to reflect current nomenclatural usage (Fricke et al. 2025). In addition, *Lampadena* aff. *jacksoni* (pl. 6, fig. 51) is classified as *Dasyscopelus* aff. *jacksoni* (Aguilera & Rodrigues de Aguilera, 2001), following the comparative myctophid morphology discussed in Lin & O'Dea (2025).

6. We corrected typographical errors in several taxonomic names, including the family name Bembropidae instead of "Brembropidae" and Gempylidae instead of "Gempilidae."

7. We also updated several names to reflect current nomenclatural usage (Fricke et al., 2025).

8. We have corrected the total otolith count from 596 to 597 to include the holotype of *P. schwarzhansi*, which was previously not included in the count.

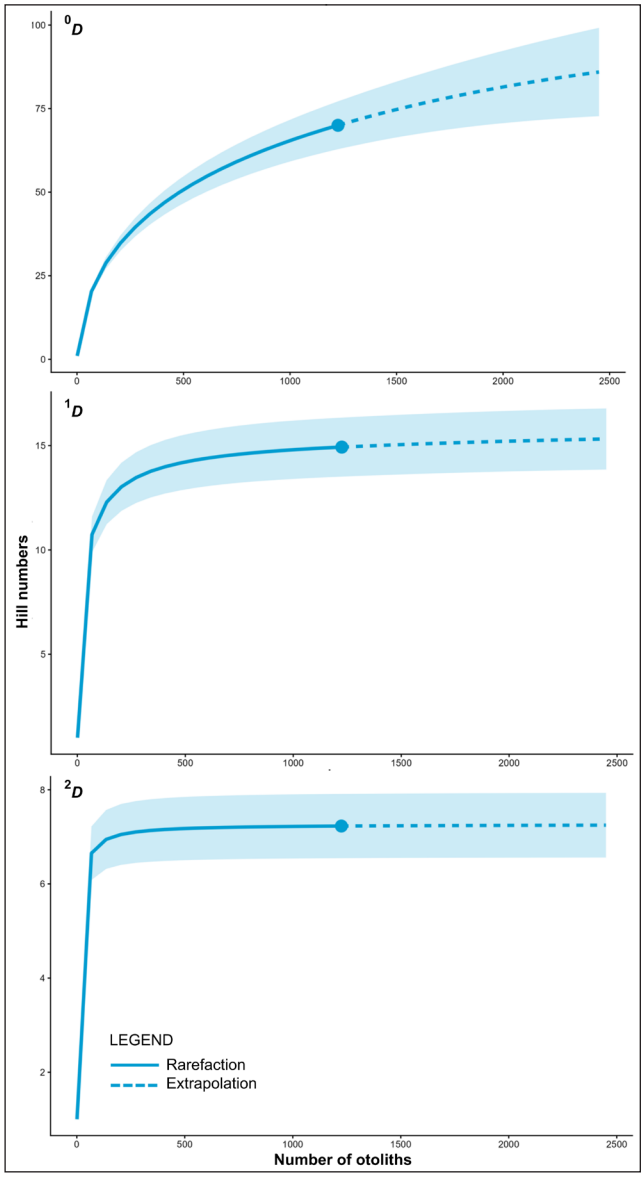

Fig. 15 - Rarefaction curves of otolith diversity (Hill numbers) from Early Pliocene marine sediments in Cabarruyan Island, northwestern Luzon Island, Philippines, including species richness (^0D), Shannon diversity (^1D), and Simpson diversity (^2D). Shaded areas represent 95% confidence intervals based on 300 bootstrap values.

Diversity and abundance

Most otoliths in this study were retrieved from Site 1 (Rarang Fishpond), and assemblage-level patterns are therefore strongly influenced by that locality (Fig. 16). Taxonomic resolution is also limited by fragmentation and abrasion, resulting in a proportion of indeterminate specimens and making observed richness conservative. Because the number of sampled localities and horizons remains limited, the present dataset should be viewed as a quantitative baseline rather than a complete inventory. Nevertheless, the recognition of 28 families substantially expands the fossil ichthyofaunal record of the Philippines. The updated compilation provided here (Tab. 1), building on van Hinsbergh and Helwerda (2019), offers a standardized taxonomic reference for future work in the Philippines and the tropical West Pacific (Kocsis et al. 2024; Mediodia et al. 2025).

At the family level, rank-abundance patterns show strong dominance by Myctophidae and Sternoptychidae, followed by Bregmacerotidae, Macrouridae, and Apogonidae (Tab. 3; Fig. 13). This overall composition is broadly consistent with the Cabarruyan Island assemblage reported by van Hinsbergh and Helwerda (2019). We note that the occurrence of new myctophid taxa in the Cabarruyan record, together with other Neogene records from the region (e.g., Lin et al. 2023), highlights substantial lanternfish diversity in the western tropical Pacific during the Pliocene. Therefore, expanded sampling from additional exposures of the otolith-bearing Pliocene clastic unit in Pangasinan will be necessary to assess spatial heterogeneity and to refine richness estimates, particularly for rare taxa.

Diversity analyses and rarefaction analyses (Fig. 14; Tab. S3) indicate that the assemblage was both rich and taxonomically complex. However, otolith density (otoliths kg^{-1} dry sediment) is significantly higher at Site 1 than at Sites 2 and 3; because density is standardized by sediment mass, this difference is unlikely to reflect sampling effort alone and may instead indicate locality-level variation in otolith concentration and/or depositional–taphonomic conditions. Additional standardized sampling at Sites 2 and 3, and from other exposures of the otolith-bearing Pliocene clastic unit in Pangasinan, will be necessary to test the robustness of site-level differences and to better constrain the rare end of the richness distribution.

Inferred paleoenvironment based on fish otoliths

The Cabarruyan assemblage is dominated primarily by mesopelagic taxa, particularly Myctophidae and Sternoptychidae, with additional contributions from Macrouridae and a minor component of shallow-water-associated groups (e.g., apogonids and gobiids). This taxonomic structure supports an open-marine setting with substantial input from the mesopelagic realm (Lin et al. 2023b). The consistent dominance of lanternfishes and other pelagic com-

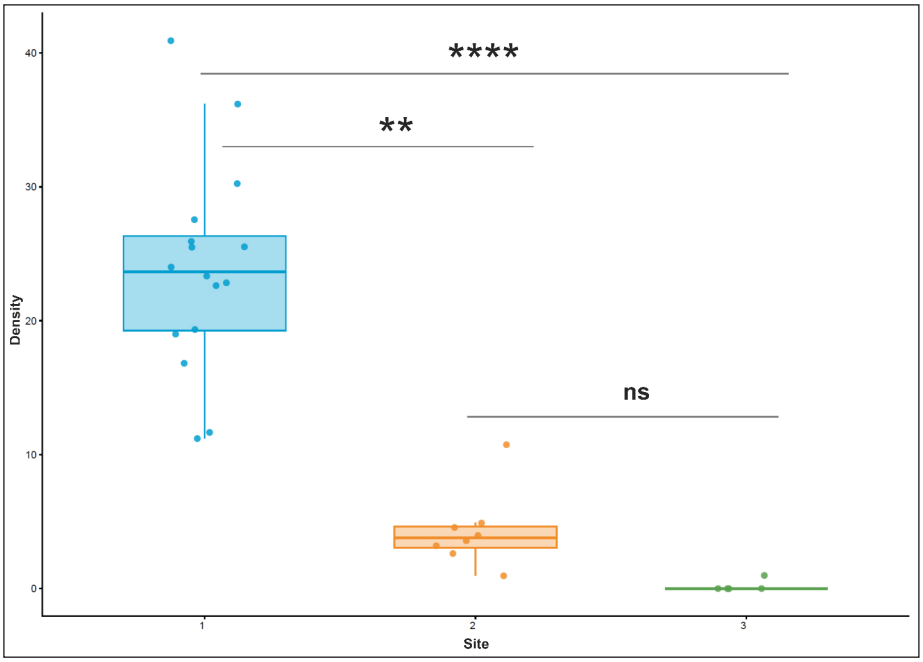

Fig. 16 - Otolith density (kg-¹) in three different sites, tested using a non-parametric workflow (Kruskal–Wallis with Dunn's post hoc comparisons, Holm-adjusted). **** denotes $p < 0.0001$; ** $p < 0.01$; ns = not significant.

ponents, together with the presence of deeper-water demersal taxa such as macrourids, is most parsimoniously interpreted as deposition on the outer shelf to upper slope, or within a setting closely connected to that bathymetric zone (Schwarzhans & Aguilera 2013; Lin et al. 2016, 2017, 2018).

The occurrence of fewer shallow-water-associated taxa alongside abundant mesopelagic elements likely reflects taphonomic mixing and transport, rather than a single uniform habitat. In outer-shelf to upper-slope settings, episodic high-energy processes can introduce shallower-water remains into more offshore depositional environments (Lin et al. 2016, 2017). We therefore interpret the assemblage as representing an open-marine outer-shelf to upper-slope setting with intermittent transport of nearshore components.

Conclusions

In this study, we document a Lower Pliocene paleoichthyological assemblage from Cabarruyan Island (Anda, Pangasinan) based on fossil otoliths. We further constrain the age of the otolith-bearing fine-grained clastic unit using calcareous nannofossil and planktonic foraminiferal biostratigraphy, indicating a late Early Pliocene age. The 1,225 recovered otoliths are assigned to at least 69 taxa across 28 families, highlighting a rich, well-diversified assemblage. Two new myctophid species are included, herein described as *Benthosema rarang* and *Myctophum luzonicum*, as well as 48 new fossil otolith records from the Philippines, significantly expanding the known otolith-based diversity of the region. The assemblage is dominated by Myctophidae and Sternoptychidae, with additional contributions from Bregmacerotidae, Macrouridae, and Apogonidae, documenting a diverse mesopelagic–demersal fauna. The taxonomic composition, together with the presence of mixed-depth elements, supports an open-marine outer-shelf to upper-slope depositional setting, with transport and mixing rather than a single uniform habitat. Collectively, these results refine the age and paleoenvironmental framework of the Cabarruyan clastic succession and provide a robust baseline for future assessments of fish paleodiversity and faunal change in the tropical West Pacific during the Neogene.

Author's contributions

This study was conceptualized by DPM, C-HL, and AGSF. Site visit and sediment collection were done by DPM, C-HL, JPB, and AGSF. Sediments were then analyzed for paleontological dating by JPB, LPdS, and AGSF. DPM and LAST processed, prepared, and imaged the otoliths. Identification was then done by DPM and C-HL. DPM performed the analysis, and JPB, LPdS, and AGSF prepared the geological setting section and performed biostratigraphic analysis. DPM, AGSF, and C-HL wrote the draft of the manuscript. All authors contributed to writing the manuscript and approved the final version.

Data Availability Statement

All materials and figured specimens have been registered and deposited in the Nannoworks Laboratory, National Institute of

Geological Sciences, University of the Philippines Diliman, Philippines, with registration numbers NIGSPAL-FISH-013 to NIGSPAL-FISH-85, and the holotypes were deposited at the National Museum of the Philippines, with registration numbers NMP-2523 and NMP-2524. All data generated in this study are included in this published article. Additional information can be requested from the corresponding author.

Acknowledgments: This study was supported by the National Science and Technology Council, Taiwan (Grant No. 111-2116-M-001-033, 112-2116-M-001-017-MY3) and Academia Sinica, Taipei, Taiwan (Career Development Award, AS-CDA-114-L04) to C-HL and the Emerging Interdisciplinary Research (EIDR) Program "Discovering the world of first hominins in the Philippines – geology, palaeoenvironment, and palaeoecology of archaic hominins in the Philippines – Project 3: Geological Environments" (OVPAA-EIDR Code EIDR-C08-008) under the Office of the Vice President for Academic Affairs of the University of the Philippines to AGSF. We thank the Mines and Geosciences Bureau of the Philippines (MGB), the National Museum of the Philippines - Division of Geology, the National Institute of Geological Sciences, and the University of the Philippines. We extend our gratitude to the Local Government Units of Pangasinan. We also thank Abigael Castro, Jaan Ruy Conrad P. Nogot, Aryssa Orven E. Martin, David Policarpio, Joeven Calvelo, Antero Borja II, Renato Bautista, Ruben Jimenez, and Chia-Hsin Hsu for their help during the collection and preparation of sediments. We would also like to thank the members of the Marine Paleontology Laboratory, especially Hsin-Wei Liu, for their support, especially during the development of the plates.

References

Agiadi K., Azzarone M., Hua Q., Kaufman D.S., Thivaiou D. & Albano P.G. (2022) - The taphonomic clock in fish otoliths. *Paleobiology*, 48(1): 154–170.

Aguilera O. & de Aguilera D.R. (2001) - An exceptional coastal upwelling fish assemblage in the Caribbean Neogene. *Journal of Paleontology*, 75(3): 732–742.

Baguio J.P., Fernando A.G. & De Silva L. (2025) - Preliminary results of the analysis of foraminiferal assemblages from Pliocene sedimentary units in Anda, Pangasinan. *5th Graduate Research Conference, National Institute of Geological Sciences, College of Science, University of the Philippines Diliman*.

Benton M.J. & Harper D.A.T. (2013) - *Introduction to paleobiology and the fossil record*. John Wiley & Sons. 608 pp.

Bolli H.M. (1970) - The foraminifera of Sites 23–31, Leg 4. *Initial Reports of the Deep Sea Drilling Project*, 4: 577–643.

Braches F. & Shutler R. (1984) - The Philippines and Pleistocene dispersal of mammals in island Southeast Asia. *Philippine Quarterly of Culture & Society*, 12(2): 106–115.

Brzobohatý R. & Nolf D. (2000). *Diaphus* otoliths from the European Neogene (Myctophidae, Teleostei). Bulletin de l'Institut royal des Sciences naturelles de Belgique: Sciences de la Terre, 70: 185–206.

Brzobohatý R. & Nolf D. (2018) - Revision of the Middle Badenian fish otoliths from the Carpathian Foredeep in Moravia (Middle Miocene, Czech Republic). *Cybium*, 42(2): 143–167.

Bureau of Mines and Geosciences (BMG) (1985) - Sheet 2969 II, geologic map of Bolinao quadrangle [Geologic map]. Bureau of Mines and Geosciences, Quezon City, Philippines.

Chao A., Chiu C.-H. & Jost L. (2014) - Unifying species diversity, phylogenetic diversity, functional diversity, and related similarity and differentiation measures through Hill numbers. *Annual Review of Ecology, Evolution, and Systematics*, 45(1): 297–324.

Chao A. & Jost L. (2012) - Coverage-based rarefaction and extrapolation: Standardizing samples by completeness rather than size. *Ecology*, 93(12): 2533–2547.

Chew Z., Hsieh E. & Lin C.-H. (2025) - Broad-spectrum fishing and small fish use in Late Neolithic Taiwan: New insights from otolith-based analysis. *Journal of Archaeological Science*, 184: 106422.

Davis M.P., Sparks J.S. & Smith W.L. (2016) - Repeated and widespread evolution of bioluminescence in marine fishes. *PLoS ONE*, 11(6): e0155154.

de Ocampo R.S. (1983) - *Plio-Pleistocene geology of Bolinao, Pangasinan and vicinities* (Geological Papers No. 2). National Museum of the Philippines. 26 pp.

Dimalanta C.B., Salapare R.C., Faustino-Eslava D.V., Ramos N.T., Queaño K.L., Yumul G.P. & Yang T.F. (2015) - Post-emplacement history of the Zambales Ophiolite Complex: Insights from petrography, geochronology, and geochemistry of Neogene clastic rocks. *Journal of Asian Earth Sciences*, 104: 215–227.

Fraser T.H. & Prokofiev A.M. (2016) - A new genus and species of cardinalfish (Percomorpha, Apogonidae, Sphaeramiini) from the coastal waters of Vietnam: luminescent or not? *Zootaxa*, 4144(2): 227–242.

Fricke R., Eschmeyer W.N. & Van der Laan R. (2025) - Eschmeyer's catalog of fishes: genera, species, references.*World Wide Web electronic publication*. https://researcharchive.calacademy.org/research/ichthyology/catalog/fishcatmain.asp. Electronic version accessed November 2025.

Helwerda R.A., Wesselingh F.P. & Williams S.T. (2014) - On some Vetigastropoda (Mollusca, Gastropoda) from the Plio-Pleistocene of the Philippines with descriptions of three new species. *Zootaxa*, 3755(2): 101–135.

Hill M.O. (1973) - Diversity and evenness: A unifying notation and its consequences. *Ecology*, 54(2): 427–432.

Hohenegger J. (2005) - Estimation of environmental paleogradient values based on presence/absence data: A case study using benthic foraminifera for paleodepth estimation. *Palaeogeography*, *Palaeoclimatology*, *Palaeoecology*, 217(1–2): 115–130.

Hsieh T.-C., Ma K.-H. & Chao A. (2016) - iNEXT: An R package for rarefaction and extrapolation of species diversity (Hill numbers). *Methods in Ecology and Evolution*, 7(12): 1451–1456.

Janssen A.W. (2007) - Holoplanktonic mollusca (Gastropoda: Pterotracheoidea, Janthinoidea, Thecosomata and Gymnosomata) from the Pliocene of Pangasinan (Luzon, Philippines). *Scripta Geologica*, 135: 29–178.

Kocsis L., Lin C.-H., Bernard E. & Johari A. (2024) - Late Miocene teleost fish otoliths from Brunei Darussalam (Borneo) and their implications for palaeoecology and palaeoenvironmental conditions. *Historical Biology*, 36(12): 2642–2676.

Lin C.-H., Brzobohatý R., Nolf D. & Girone A. (2017) - Tortonian teleost otoliths from northern Italy: Taxonomic synthesis and stratigraphic significance. *European Journal of Taxonomy*, 322: 1–44.

Lin C.-H. & Chang C.-W. (2012) - Otolith atlas of Taiwan

fishes. National Museum of Marine Biology and Aquarium. 416 pp.

Lin C.-H. & Chien C.-W. (2021) - Late Miocene otoliths from northern Taiwan: Insights into the rarely known Neogene coastal fish community of the subtropical northwest Pacific. *Historical Biology*, 34(2): 361–382.

Lin C.-H., Chien C.-W., Lee S.-W. & Chang C.-W. (2021) - Fish fossils of Taiwan: a review and prospection. *Historical Biology*, 33(9): 1362–1372.

Lin C.-H., De Gracia B., Pierotti M.E.R., Andrews A.H., Griswold K. & O'Dea A. (2019) - Reconstructing reef fish communities using fish otoliths in coral reef sediments. *PLoS ONE*, 14(6): e0218413.

Lin C.-H., Girone A. & Nolf D. (2015) - Tortonian fish otoliths from turbiditic deposits in Northern Italy: Taxonomic and stratigraphic significance. *Geobios*, 48(3): 249–261.

Lin C.-H., Girone A. & Nolf D. (2016) - Fish otolith assemblages from Recent NE Atlantic sea bottoms: A comparative study of palaeoecology. *Palaeogeography*, *Palaeoclimatology*, *Palaeoecology*, 446: 98–107.

Lin C.-H. & O'Dea A. (2025) - Remarkable dominance of myctophid otoliths in Upper Miocene Chagres Formation, Caribbean Panama. *PeerJ*, 13: e20155.

Lin C.-H., Steurbaut E. & Nolf D. (2024) - Early Eocene fish otoliths from the eastern and southern USA. *European Journal of Taxonomy*, 935: 203–240.

Lin C.-H., Taviani M., Angeletti L., Girone A. & Nolf D. (2017) - Fish otoliths in superficial sediments of the Mediterranean Sea. *Palaeogeography*, *Palaeoclimatology*, *Palaeoecology*, 471: 134–143.

Lin C.-H., Wei C.-L., Ho S.L. & Lo L. (2023a) - Ocean temperature drove changes in the mesopelagic fish community at the edge of the Pacific Warm Pool over the past 460,000 years. *Science Advances*, 9(27): eadf0656.

Lin C.-H., Wu S.-M., Lin C.-Y. & Chien C.-W. (2023b) - Early Pliocene otolith assemblages from the outer-shelf environment reveal the establishment of mesopelagic fish fauna over 3 million years ago in southwestern Taiwan. *Swiss Journal of Palaeontology*, 142: 12.

Martin R.P., Olson E.E., Girard M.G., Smith W.L. & Davis M.P. (2018) - Light in the darkness: new perspective on lanternfish relationships and classification using genomic and morphological data. *Molecular Phylogenetics and Evolution*, 121: 71–85.

Mediodia D., Castro A., Tablizo M., Policarpio D., Calvelo J., Baguio J.P., Borja A. II, Lin C.-H. & Fernando A.G. (2025) - Paleoichthyology in the Philippines: A review of Cenozoic fish fossils with insights on its current status and future opportunities. *Geobios*, 88: 163–174.

Mines and Geosciences Bureau (MGB) (2010) - *Geology of the Philippines* (2nd ed.). Mines and Geosciences Bureau, Department of Environment and Natural Resources, Manila, Philippines.

Mitsui S., Lin C.-H., Taru H. & Shibata K. (2023) - Fish otolith record reveals possible tropical-subtropical fish community in temperate Japan during the exceptionally warm Last Interglacial period. *Historical Biology*, 36(5): 1007–1027.

Mitsui S., Taru H., Ohe F., Lin C.-H. & Strüssmann C.A. (2021) - Fossil fish otoliths from the Chibanian Miyata Formation, Kanagawa Prefecture, Japan, with comments on the paleoenvironment. *Geobios*, 64: 47–63.

Nafpaktitis B.G. & Paxton J.R. (1968) - Review of the lanternfish genus *Lampadena* with a description of a new species. *Contributions in Science*, 138:1–29.

Nelson J.S., Grande T.C. & Wilson M.V.H. (2016) - *Fishes of the world* (5th ed.). John Wiley & Sons. 752 pp.

Ng S.-L., Lin C.-H., Liu K.-M. & Joung S.-J. (2024) - New records of three mesopelagic fish species from southwestern Taiwan. Thalassas: *An International Journal of Marine Sciences*, 40: 81–90.

Nolf D. (2013) - *The diversity of fish otoliths, past and present*. Royal Belgian Institute of Natural Sciences, Brussels. 222 pp.

Nolf D. & Cappetta H. (1989) - Otolithes de poissons pliocènes du Sud-Est de la France. *Bulletin de l'Institut Royal des Sciences Naturelles de Belgique*, *Sciences de la Terre*, 58: 209–271.

Papazzoni C.A. & Trevisani E. (2006) - Facies analysis, palaeoenvironmental reconstruction, and biostratigraphy of the "Pesciara di Bolca" (Verona, northern Italy): An early Eocene Fossil-Lagerstätte. *Palaeogeography*, *Palaeoclimatology*, *Palaeoecology*, 242(1–2): 21–35.

Ohe F. (1983) - On the otoliths of deep water fishes from Pliocene Hijikata mud formation exposed in the southern part of Kakegawa Prefecture, central Japan. *Bulletin of the Senior High School Attached to the Aichi University*, 10: 1–54.

Ohe F. (1985) - *Marine fish-otoliths of Japan*. The Senior High School Attached to the Aichi University Education. 184 pp.

Peña R.E. (2008) - *Lexicon of Philippine stratigraphy*. Geological Society of the Philippines, Inc., Mandaluyong City, Philippines. 364 pp.

Přikryl T., Castro A., Fernando A.G., Nogot J.R.C., Magtoto C., Garas K., Mediodia D. & Lin C.-H. (2025) - Fossil fish assemblage of the Laguna Formation, Philippines: unveiling the uniqueness of Pleistocene freshwater ecosystems in Southeast Asia. *Swiss Journal of Palaeontology*, 144: 5.

Queaño K.L., Dimalanta C.B., Yumul G.P., Marquez E.J., Faustino-Eslava D.V., Suzuki S. & Ishida K. (2016) - Stratigraphic units overlying the Zambales Ophiolite Complex (ZOC) in Luzon, (Philippines): Tectonostratigraphic significance and regional implications. *Journal of Asian Earth Sciences*, 142: 20–31.

Rangin C. (1991) - The Philippine Mobile Belt: a complex plate boundary. *Journal of Southeast Asian Earth Sciences*, 6(3–4): 209–220.

Rivaton J. & Bourret P. (1999) - *Otoliths of the Indo-Pacific fishes*. Documents Scientifiques et Techniques, Nouméa, Nouvelle-Calédonie. 378 pp.

Schwarzhans W. (1999) - A comparative morphological treatise of recent and fossil otoliths of the order Pleuronectiformes. Piscium Catalogus: Part Otolithi piscium 2, Verlag Dr. Friedrich Pfeil, München. 392 pp.

Schwarzhans W. (2013a) - Otoliths from dredges in the Gulf of Guinea and off the Azores - An actuo-paleontological case study. *Palaeo Ichthyologica*, 13: 7–40.

Schwarzhans W. (2013b) - A comparative morphological study of the recent otoliths of the genera *Diaphus*, *Idiolychnus* and *Lobianchia* (Myctophidae). *Palaeo Ichthyologica*, 13: 41–82.

Schwarzhans W. (2014) - Head and otolith morphology of the genera *Hymenocephalus*, *Hymenogadus* and *Spicomacrurus* (Macrouridae), with the description of three new species. *Zootaxa*, 3888(1): 1–73.

Schwarzhans W. (2019) - Reconstruction of the fossil marine bony fish fauna (Teleostei) from the Eocene

to Pleistocene of New Zealand by means of otoliths. *Memorie della Società Italiana di Scienze Naturali e del Museo di Storia Naturale di Milano*, 46: 3–326.

Schwarzhans W. & Aguilera O. (2013) - Otoliths of the Myctophidae from the Neogene of tropical America. *Palaeo Ichthyologica*, 13: 83–150.

Schwarzhans W. & Bratishko A. (2011) - The otoliths from the middle Paleocene of Luzanivka (Cherkasy district, Ukraine). *Neues Jahrbuch für Geologie und Paläontologie*, 261(1): 83–110.

Schwarzhans W. & Ohe F. (2019) - Lanternfish otoliths (Teleostei, Myctophidae) from the Pliocene and Pleistocene of Japan. *Rivista Italiana di Paleontologia e Stratigrafia*, 125(2): 355–400.

Schwarzhans W. & Prokofiev A.M. (2017) - Reappraisal of *Synagrops* Günther, 1887 with rehabilitation and revision of *Parascombrops* Alcock, 1889 including description of seven new species and two new genera (Perciformes: Acropomatidae). *Zootaxa*, 4260(1): 1–74.

Schwarzhans W., Brzobohatý R. & Radwańska R. (2020) - Goby otoliths from the Badenian (middle Miocene) of the Central Paratethys from the Czech Republic, Slovakia and Poland: A baseline for the evolution of the European Gobiidae (Gobiiformes; Teleostei). *Bollettino della Società Paleontologica Italiana*, 59(2): 125–173.

Schwarzhans W., Ohe F., Tsuchiya Y. & Ujihara A. (2022) - Lanternfish otoliths (Myctophidae, Teleostei) from the Miocene of Japan. *Zitteliana*, 96: 103–134.

Smale M.J., Watson G. & Hecht T. (1995) - Otolith atlas of southern African marine fishes. J.L.B. Smith Institute of Ichthyology. 253 pp.

Srinivasan M.S., Kennett J.P. & Rodda P. (1981) - Late Neogene planktonic foraminiferal biostratigraphy, Suva, Fiji. *Journal of Paleontology*, 55(4): 858–867.

Su Y., Lin H.-C. & Ho H.-C. (2023) - New records of two cusk eels of the genus *Neobythites* from Taiwan, with a northward range extension of *N. australiensis* Nielsen, 2002 (Actinopterygii: Ophidiiformes: Ophidiidae). *Acta Ichthyologica et Piscatoria*, 53: 243–251.

van der Laan R., Eschmeyer W.N. & Fricke R. (2014) - Family-group names of recent fishes. *Zootaxa*, 3882(1): 1–230.

van Hinsbergh V.W.M. & Helwerda R.A. (2019) - Fish otoliths from the Cabarruyan Piacenzian–Gelasian fauna found in the Philippines. *Zootaxa*, 4563(3): 401–443.

Yang T.F., Lee T., Chen C.-H., Cheng S.-N., Knittel U., Punongbayan R.S. & Rasdas A.R. (1996) - A double island arc between Taiwan and Luzon: consequence of ridge subduction. *Tectonophysics*, 258: 85–101.